SpaceOps-2025, ID #228

JWST Fine Guidance Sensor Optimizations and Improvements since Launch

Gerald Warner[a], Neil Rowlands[a], Bruce Barringer[b], Nicholas Bond[c,d], Pierre Chayer[b], Audrey DiFelice[b], Jean Dupuis[e], Sherie Holfeltz[b], S. Tony Sohn[b], Scott D. Lambros[c,f], Amanda Marrione[b], Christopher D. Moller[c,f], Ed Nelan[b], M. Begoña Vila[c,g], Jared Yeates[a], Julia Zhou[e].

[a] Honeywell Aerospace, 400 Maple Grove Rd, Kanata, ON, Canada K2V 1B8

[b] Space Telescope Science Institute, 3700 San Martin Dr, Baltimore, MD 21218

[c] NASA's Goddard Space Flight Center, 8800 Greenbelt Rd, Greenbelt, MD 20771

[d] Adnet Systems Inc, 6720B Rockledge Dr #504, Bethesda, MD 20817

[e] Canadian Space Agency/Agence Spatiale Canadienne, 6767 Rte de l'Aéroport, Saint-Hubert, QC J3Y, 8Y9, Canada

[f] Aerodyne Industries, 7701 Greenbelt Road, Suite 300, Greenbelt, MD 20770

[g] KBR, 7701 Greenbelt Rd #400, Greenbelt, MD 20770

ABSTRACT

After launch and throughout operations multiple optimizations to improve the Fine Guidance Sensor (FGS) performance of the James Webb Space Telescope (JWST) were implemented. Some of the optimizations were planned based on prior knowledge from ground testing and simulation, and some of them were determined during operations in response to unexpected conditions. This paper will provide examples of both, including: the selection and classification of pixels for inclusion on the bad pixel map and the cadence for bad pixel map updates; the determination of overall instrument throughput required to tune the range of dim and bright guide star magnitudes to utilize from the Guide Star Catalog; confirmation and calibration of the detector saturation level and effective dynamic range available for measuring star brightness; Photo Response Non-Uniformity (PRNU) evaluation and identification of shortcomings in the pre-launch ground calibration of PRNU with diffuse illumination relative to on-orbit measurements of point sources; trade-offs between commanded parameters versus flight software data table parameter updates to support operations; and improvements on the operational requirements in bright crowded fields in particular towards the center of the galaxy.

Many of these optimizations involve interactions with other subsystems such as: the Attitude Control System (ACS) to determine the allowed pointing inaccuracy of the Observatory slew when entering different Guider modes (Identification, Acquisition, Track) for FGS to identify the correct Guide Star; the Operations Script Subsystem (OSS) which commands the handshake between FGS and ACS and implements parameter updates as needed for some of the operations; and the Guide Star Catalog to indicate exclusion areas, and to correct for misclassified or duplicate objects. Optimizations also include the optical distortion and geometric calibrations captured in the Science Instruments Aperture Files for accurate pointing on the other Science Instruments' fields of view and during dithers and target acquisitions.

Throughout operations several possible flight software algorithm optimizations have also been identified, related to the identification of very bright stars which saturate the detector readout; the extrapolated placement of fine guide sub-windows while ignoring bad centroids; and the photometric bad pixel replacement algorithm and these will also be summarized.

Keywords: James Webb Space Telescope, Fine Guidance Sensor, Bad Pixel Map, Guide Star Catalog, Flight Software, Bright Crowded Fields

Acronyms

ACQ - Acquisition
ACS – Attitude Control System
ADU – Analog to Digital Unit
BCF – Bright Crowded Field
BPM – Bad Pixel Map
CDS – Correlated Double Sample
CSA – Canadian Space Agency
FFM – Fine Focus Mechanism
FG – Fine Guide
FGS – Fine Guidance Sensor
FOT – Flight Operations Team
FOV – Field of View
FSM – Fine Steering Mirror
FSW – Flight Software
FWHM – Full Width Half Max
GS – Guide Star
GSC – Guide Star Catalog
GSSS – Guide Star Selection System
HST – Hubble Space Telescope
ID – Identification
IPC – Inter-Pixel Capacitance
JWST – James Webb Space Telescope
NEA – Noise Equivalent Angle
NIRISS – Near Infrared Imager and Slitless Spectrograph
NRC – National Research Council (Canada)
OSS – Operations Script Subsystem
OTE – Optical Telescope Element
OTIS – Optical Telescope Element and Integrated Science Instrument Module
PPRS – Post Pixel Readout Signal
PRNU – Photo-Response Non-Uniformity
PSF – Point Spread Function
RC – Resistor/Capacitor
RTN – Random Telegraph Noise
SI – Science Instrument
STScI – Space Telescope Science Institute
TRK - Track
UTR – Up The Ramp

1. Introduction

The James Webb Space Telescope (JWST) is a large aperture optical and infrared telescope (~6.5 meters in diameter) developed by an international team led by the United States National Aeronautics and Space Administration (NASA) with partners the Canadian Space Agency (CSA) and the European Space Agency (ESA). The JWST Observatory was successfully launched by an Ariane V launcher (VA256) provided by ESA on December 25th, 2021. On January 23rd after the third successful mid-course correction maneuver, the JWST Observatory entered into a halo orbit around the Sun-Earth L2 Lagrange point located approximately 1.5 million km from earth in the anti-solar direction. JWST enables the study of the very first stars and galaxies born after the Big Bang, of planets (both in our own solar system and exoplanets), and the process of formation of stars and galaxies. A logical complement to the Hubble Space Telescope (HST), it focuses on deep imaging and multi-object spectroscopy in the near-infrared and thermal infrared portions of the spectrum [1][2].

The Fine Guidance Sensor (FGS) along with the Near Infrared Imager and Slitless Spectrograph (NIRISS) form the Canadian contribution to the JWST mission [3][4]. This paper considers specifically several of the post-launch optimizations and performance improvements made for the FGS instrument. The FGS consists of three main functional elements (Optical Assembly, Electronics, and Flight Software) as shown in the overall block diagram of Figure 1. From a post-launch perspective, performance optimizations are addressed in terms of Flight Software (FSW) changes (comprising both core algorithm/source code modifications and updates to calibration tables and onboard data table parameters), determined in conjunction with ground-based analysis and data processing techniques.

After JWST was launched, FGS Commissioning activities took place with direct 24/7 on console support at the Science Operations and Control Center at the Space Telescope Science Institute (STScI) in Baltimore from January 28th to the end of June 2022. The FGS/NIRISS Commissioning team included personnel from Honeywell, CSA, NASA's Goddard Space Flight Center, Université de Montréal, Canadian National Research Council's Herzberg Astronomy & Astrophysics Research Centre, CSA supported team members based at STScI, along with STScI Flight Operations

Team (FOT) members and STScI NIRISS science team members. Key milestones in the FGS/NIRISS Commissioning are shown in Table 1. After the Commissioning phase, the Observatory entered into its primary mission phase of scientific observations. Both phases provided insight into the instrument behaviour and yielded important data which helped to facilitate the ongoing efforts to optimize performance which will be described in this paper.

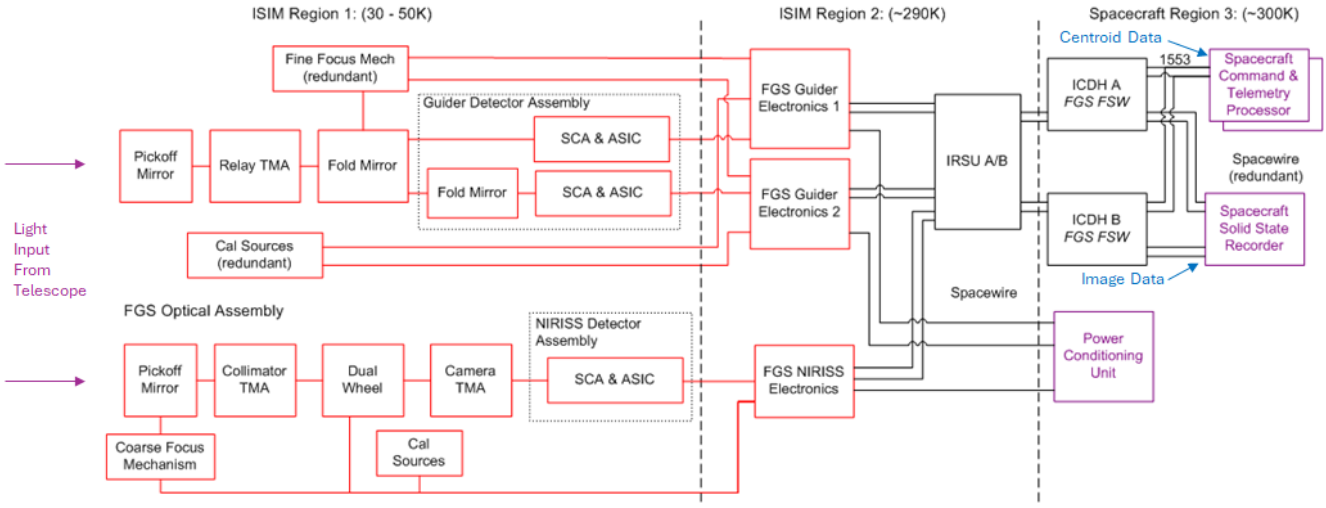

Figure 1: FGS Components Block Diagram

Table 1: FGS Commissioning Milestones

Milestone	Date	Optics Bench Temperature
FGS & NIRISS power on	January 28th, 2022	
Functional and aliveness tests completed	February 10th, 2022	75K
First successful closed loop guiding (track mode)	February 14th, 2022	65K
First successful fine guiding	March 12th, 2022	46K
Moving target observation successful on first attempt	May 3rd, 2022	40K
All four NIRISS science modes declared ready for science observations (the first Science Instrument commissioned)	June 22nd, 2022	40K

2. Focus and Optical Distortion

FGS focus evaluation was a planned Commissioning activity. Focus can be adjusted onboard using the FGS Fine Focus Mechanism (FFM), which moves the FGS focus mirror along a translational stage within the Guider optical chain. This mirror is situated before the optical split to the Guider 1 and Guider 2 detector channels, so the same mechanism determines the focus for both guiders.

The standard measure for FFM position is referenced in "mm OTE", which represents a conversion of the translational mechanism motor steps into the effective displacement in the Optical Telescope Element (OTE) space. Considerable effort was undertaken during ground testing to select the optimal pre-launch FFM focus position, or "best focus". Note that this need not necessarily correspond to the location which produces the "sharpest" focus of an imaged star on the Guider detectors, as in fact the FGS centroiding algorithm performs best when stars are at

least slightly defocused. An optimal "best focus" for Guide Star centroiding is in the range of 1.5-1.8 pixels full width half max (FWHM), or 65-75% in 3x3 pixel ensquared energy.

At launch, the Guider FFM "best focus" location was set to +3.20 mm OTE. It was not known if launch vibrations might introduce disturbance to the FFM mechanism position, or if the use of "real stars" with realistic point source characteristics across the different spectral types might require adjustment of the Guider focus. Commissioning plans were set to evaluate Guider focus throughout the primary mirror alignment stages, and to perform a final Guider focus sweep to determine if the FFM position should be updated prior to commencing normal operations.

The Guider focus was evaluated using background star fields at the conclusion of each of the Observatory primary mirror segment alignment stages in March and April, 2022. Subsequently, when primary mirror alignment was completed, a full Guider FFM focus sweep was conducted, imaging a background star field while the FFM was stepped across an extended portion of its travel range.

The mean FWHM of a group of 15-20 selected stars in each field was plotted against the FFM position, as shown in Figure 2. As the curves indicate, the minimum FWHM (sharpest focus) was reproduced very near to the pre-launch determined location of +3.20 mm OTE. However, particularly for Guider 2, this resulted in a mean FWHM below 1.5 pixels. This raised the concern that perhaps the focus would be too sharp for optimal centroiding during Guider operations if the focus was left in that configuration. The cause for sightly sharper focus on orbit was believed to be due to a combination of imaging stars as true point sources plus the tendency for stars of non-red spectral types to have slightly lower FWHM. These conditions represented a difference from the ground-based observations with artificial light sources at fixed wavelengths.

A final decision was made to slightly adjust the FFM "best focus" location to +2.20 mm OTE, as indicated by the red vertical line in Figure 2. This has the effect of very slightly defocusing the instruments, which will tend to spread star energy better across the detector pixel grid and allow slightly improved centroiding during Guider operations for a wider range of stellar spectral classes. The choice also biases the FFM setting closer to the center of its travel range. It is not anticipated that the focus position will ever need to be re-adjusted over the remaining JWST mission life.

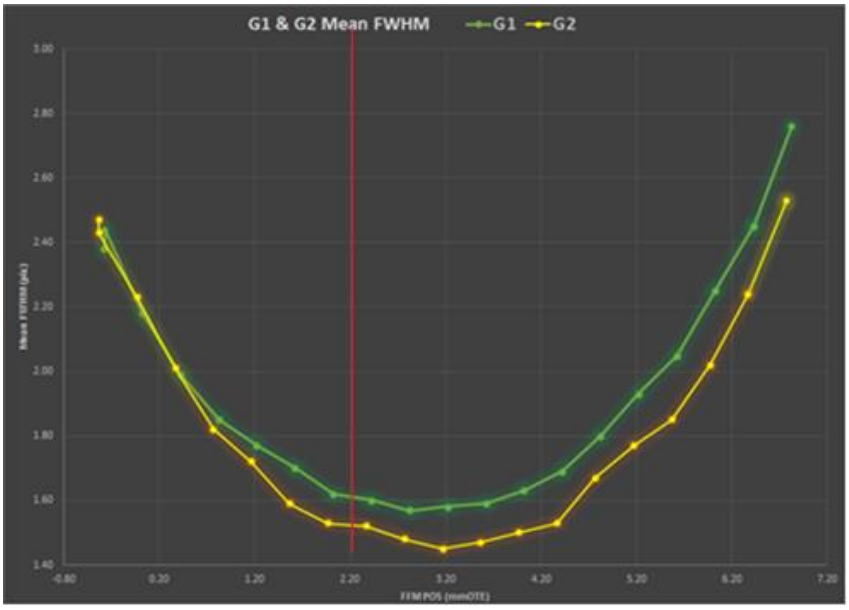

Figure 2: Guider 1 and Guider 2 FFM Best Focus Determination

Note that at the time of performing the "best focus" adjustment during Commissioning, the Guider 1 focus position was reading +3.284 mmOTE, and the desired -1.0 mm OTE adjustment was entered as a "delta" move of the FFM. As a result, the achieved FFM position was 2.289 mm OTE, which is closer to +2.30 mm OTE than to the analytical derived target of +2.20 mm OTE. There was no reason based on the focus curve to try to correct for this on orbit. A recent reading of the FFM location in Normal Operations returned a value of +2.321 mm OTE on Guider 1 and +2.293 mm OTE on Guider 2. (Although the same mechanism and physical mirror position applies to both Guiders, the subsequent resolver readout and coordinate conversion yields a slightly different number for each instrument).

Another planned optical calibration during Commissioning to optimize Guider performance involved mapping the geometrical optical distortion and plate scale in order to generate updates to the onboard flight software correction tables. These correction tables are necessary in order to accurately convert measured star positions in the Guider detector pixel coordinate grid to locations in a global undistorted reference frame. The distortion measurements were made in early May, 2022, using an astrometric star field in the Large Magellanic Cloud derived from HST observations in support of the JWST mission.

The distortion field is fitted with a two-dimensional polynomial whose coefficients are stored in instrument flight software data tables. In comparing the distortion solutions between the Commissioning result and the original solution from ground-based testing prior to launch, the maximum differences were about 0.4 arcsec for Guider 1 and 0.22 arcsec for Guider 2. These differences across the field are illustrated by the plots in Figure 3. Meanwhile, the overall average pixel plate scale was reduced for Guider 1 from 69.28 mas/pix to 69.14 mas/pix, a reduction of 0.19%. For Guider 2 the reduction was 0.13% from 68.90 mas/pix to 68.81 mas/pix.

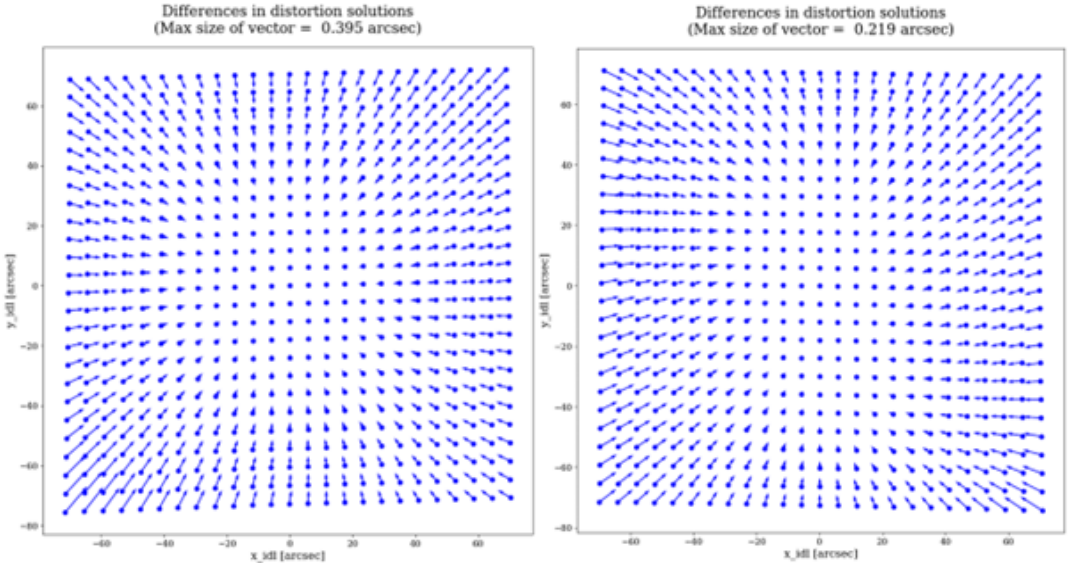

Figure 3: Guider 1 (left) and Guider 2 (right) Geometric Distortion Solution Differences

3. FGS Bad Pixel Maps (BPMs)

The JWST FGS detectors must be continually monitored for the presence of bad pixels. Bad pixels are capable of interfering with Guider operations. Bad pixels could cause failure in Identification (ID) or Acquisition (ACQ) modes if mistaken for Guide Stars, and they could cause inaccurate centroids in Track or Fine Guide modes leading to corruption of the dynamic Observatory ACS J-Frame coordinate transform matrix between the FGS and spacecraft reference frames. The FGS flight software utilizes mappings of the locations of known bad pixels and will automatically replace pixel counts in Guider mode image data to mitigate against potential interference. The maps

are loaded to instrument EEPROM and accessed by the FGS flight software during instrument initialization and operation.

Data tables containing the locations of known bad pixels on the two FGS detectors (Guider 1 and Guider 2) were generated and maintained throughout the ground cryogenic test phase prior to JWST launch. This process tended to be very "all-inclusive", identifying and categorizing pixel behaviours based on a wide range of characteristics. Pixels could be marked "bad" based on many different criteria, including high dark current, excess read noise, and low photosensitivity.

Aside from a very small number of completely "dead" pixels, most bad pixel characteristics can only be identified when the detectors are operating at their designed cold operating plateau temperature of 40 Kelvin (K). The H2RG IR detector behaviour is very sensitive to operating temperature. The final 40 K ground images used as inputs to the FGS bad pixel maps were taken during the OTIS cryogenic test campaign in 2017, while JWST was launched at the end of 2021. The bad pixel population had been previously observed to change slightly (< 1%) with thermal cycling and with accumulated radiation damage, so it was anticipated that after the intervening four years, an early on-orbit update would be necessary as part of the Commissioning phase in order to ensure optimal Guider performance.

It was not known how frequently subsequent updates to the on-orbit BPMs might be required. Monitoring the evolution of the bad pixel population and developing a process to manage the BPMs was an anticipated Commissioning analysis activity, however the finer details of implementation required gaining actual experience with on-orbit observations. One main complication to developing this process was that during normal FGS operations on orbit, the Guiders would only be imaging in the subarray readout modes regularly used during ID, ACQ, Track, and Fine Guide (FG) modes. These modes necessarily take short integrations of only selected portions of the detector arrays. And the images produced would contain background star fields as well. Therefore, the process for identifying bad pixels on-orbit would be quite different from that taken during ground testing when long integrations with completely dark backgrounds were available.

A proposed methodology was developed prior to launch for using ID strip images (the longest FGS integration times regularly available) across several different observations. Utilizing several different observations each at different Observatory pointings was necessary in order to be able to remove all background celestial objects, while any bad pixels remained in fixed locations on the detectors. This process was gradually refined and automated over the course of Commissioning and early normal operations.

At JWST launch, the Guider BPMs had already undergone numerous revisions and updates throughout the ground detector characterization and cryogenic test phases, resulting in an initial "Rev 64" version loaded prior to launch and designated for initial on-orbit FGS operation at 40K. In this initial on-orbit revision of the BPMs, there were a total of 11919 bad pixels of various types identified on the Guider 1 detector (representing 0.285% of the active pixel area) and 21508 bad pixels identified on the Guider 2 detector (representing 0.515% of the active pixels). Figure 4 shows these initial BPMs with bad pixels in black against a white background representing good pixels on the array.

Most bad pixels in the initial Guider BPMs fell into one of three categories: a) "RC" pixels, b) "PPRS" neighbours to RC pixels, and c) "RTN" pixels [5].

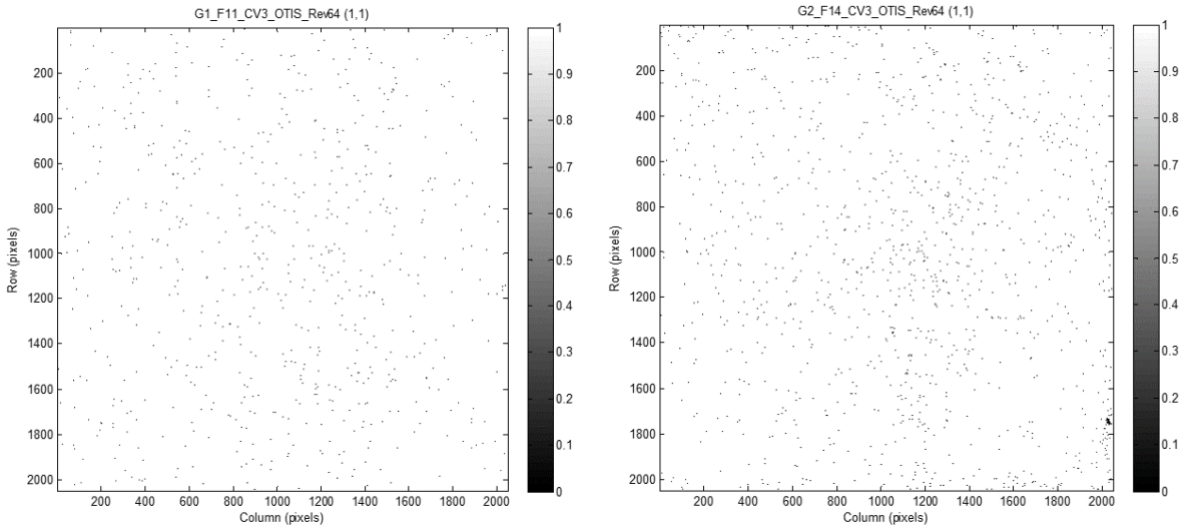

Figure 4: FGS Bad Pixel Maps at Launch (Rev 64). Left: Guider 1 initially had 11,919 bad pixels (0.285%). Right: Guider 2 initially had 21,508 bad pixels (0.515%).

RC pixels are malfunctioning pixels which show an exponential rise in dark signal over time. They were called "RC" because their signal integration can be modeled with the same kind of exponential function as the charge vs. time curve of an electrical R-C circuit. RC pixels can have a very wide range of time constants. Some saturate almost immediately on the Guider detectors, even at very short integration times. Others show counts increasing much more gradually over time. RC pixels are relatively easy to monitor during FGS operations, as they typically show as brighter or "hot" pixels against the darker background star fields. Figure 5 illustrates a variety of RC pixel counts rising over successive integrations from a dark ground test.

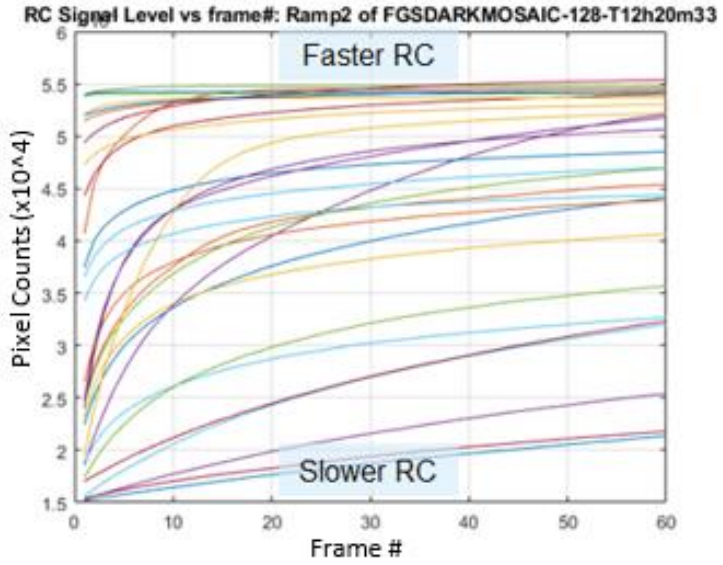

Figure 5: Sample RC Pixel Characteristics from a dark ground test

The faster RC pixels will typically saturate and produce large signals in FGS detector readouts. They also tend to produce an effect termed "post pixel readout signal" or PPRS which occurs when some of the charge from a bright

pixel is "smeared" over into the readout of the next pixel on the array along the readout direction. This is an additive effect to the usual inter-pixel capacitance (IPC) which is also observed at a lower order on the FGS detectors. In practice, what happens for a bright RC pixel is that it may produce a "+" shape on the detector; a bright central RC pixel will have a neighbour pixel in the readout direction with elevated counts, along with some slightly elevated IPC pixels in the other 3 nearest neighbours. Figure 6 illustrates this effect. (Note that in full-frame or strip imaging, the FGS detector readout direction alternates between each 512-column amplifier channel).

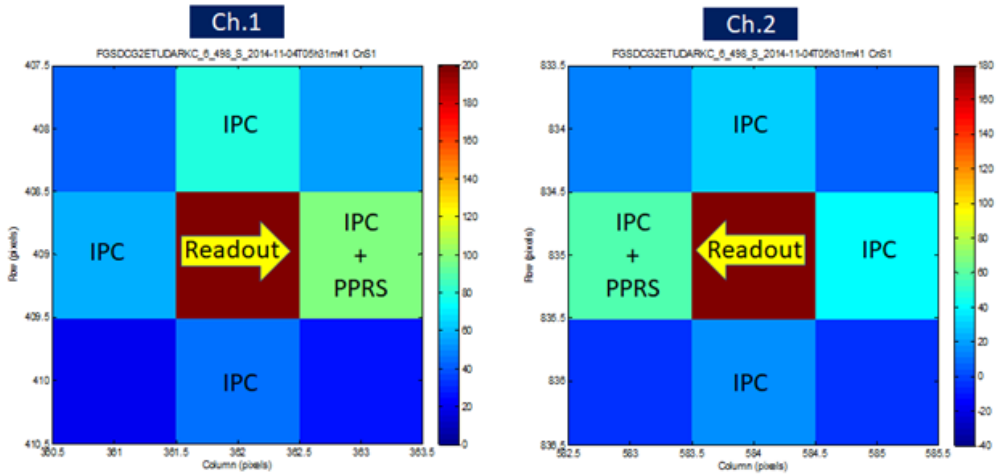

Figure 6: PPRS and IPC pixels surrounding a central RC Pixel in multi-channel FGS readout

RTN or Random Telegraph Noise pixels are believed to occur when there is an electron trap in the channel of the pixel buffer MOSFET which modulates its transconductance. This produces a "random" transition between output values for that pixel, typically with a fixed amplitude and a characteristic frequency of occurrence. Figure 7 illustrates the typical behaviour of a RTN pixel on the left in terms of the CDS counts recorded while differencing successive frames read out up-the-ramp (UTR), compared to the corresponding result for a normal pixel. Note that the RTN effect typically produces a maximum amplitude below 150 counts. Most RTN pixel amplitudes are on the order of 75 counts or lower, however.

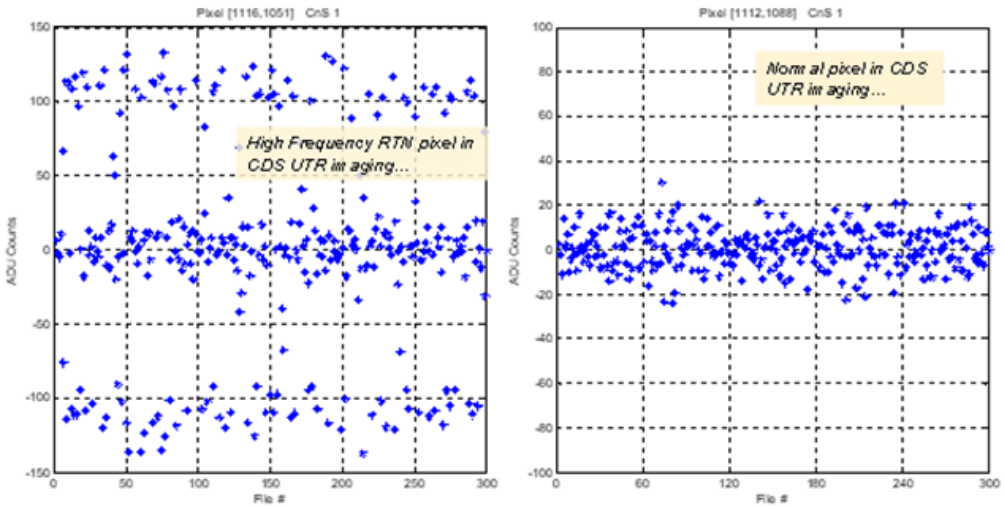

Figure 7: RTN Pixel counts (left) vs. Normal Pixel (right)

The first FGS bad pixel map update during Commissioning was completed on May 2, 2022. Soon after the end of Commissioning a monthly cadence to upload new bad pixel maps on board was established – with typically ~ 30-50 new bad pixels found per guider each month due to ongoing radiation impacts damaging individual pixels. The process involved evaluating groups of ID strip images from 10 distinct observations at different pointings, and typically only finding new RC or "hot" pixels evident in the image data. Figure 8 shows the bad pixel population growth rate in several of the early on orbit BPM updates.

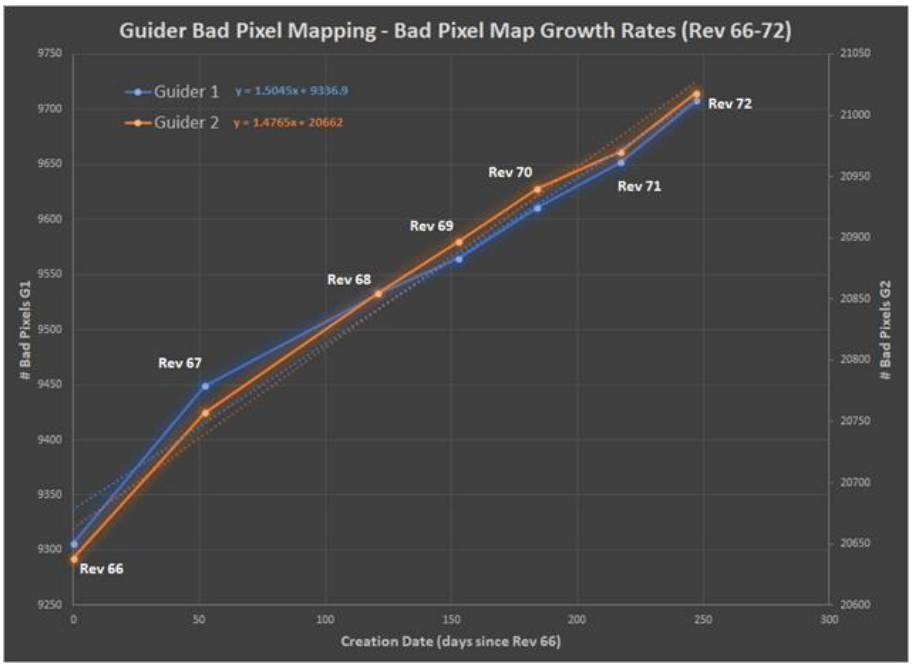

Figure 8: Growth Rates of Bad Pixels During Early FGS Operations

However, as normal operations proceeded, several instances occurred where a pixel which was not in the BPM caused Visit failures in Track or Fine Guide operations. Often, this turned out to be a PPRS neighbour to a RC pixel which was itself in the map. This often resulted in a Guider "locking on" to the bad pixel instead of the desired Guide Star, when the bad pixel had a higher peak pixel count. This returned an erroneous Guide Star centroid position, and ultimately produced a corruption of the J-Frame coordinate transformation carried by the Observatory ACS. This type of scenario resulted in several skipped science observations before a correction to the transformation matrix was applied, so the disruption to JWST operations in these instances was significant.

During Guider operations, the Guide Star Selection System will normally try to pick the brightest available Guide Star from the Guide Star Catalog. However, in some fields only a dim star is available. A typical lower count rate for the dimmest stars FGS can detect is around 15,000 counts/s in a 3x3 pixel window. In Track mode, this corresponds to 15,000 counts/s * 0.02508 s integration time = 376 counts.

Depending on how a star lands upon the FGS detector pixel grid, it may be pixelated with energy concentrated into a central single bright pixel, or energy may land on a pixel boundary and be distributed more across multiple pixels. This variability is illustrated in the two images of the same star in Figure 9. On the left, the Guide Star energy peaks in a central pixel. On the right, the same energy lands on a pixel boundary and is spread across multiple pixels. The way the star energy spreads itself across the pixel grid is often referred to as the "point spread function" or PSF. A "well peaked" PSF may have up to around 40% of the total star energy in the central peak pixel. A "less peaked" PSF could have only 20% in the peak pixel.

So for a dim Guide Star with just 376 total counts, 20% in the peak pixel would be around 75 counts. The FGS centroiding algorithm finds the peak pixel in the image area to use as the basis for its centroiding process. If any other pixel in the image area shows a count greater than the peak pixel of the Guide Star, then a centroid will be computed around that other pixel instead of the Guide Star. This is the basis for the observed failures and J-Frame corruptions encountered during early normal operations. Sometimes a PPRS pixel which was not in the BPM had counts greater than the peak pixel of a dim Guide Star, and the Track or Fine Guide algorithms would then center on this PPRS pixel instead of on the peak of the target Guide Star. This would then corrupt the ACS attitude solution thereafter.

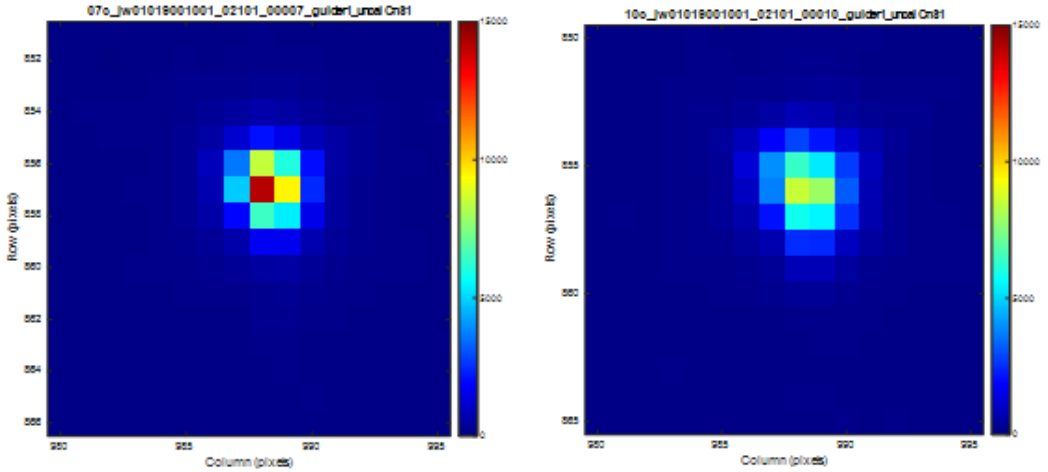

Figure 9: Two Images of the same star: Sharply peaked PSF (left) vs. Distributed PSF (right)

The methodology for adding PPRS neighbour pixels to the BPMs from on-orbit analysis was therefore revisited. The nature of how PPRS pixels could be identified and included in the BPMs was investigated.

Due to the short integration times available during Guider operations, it was difficult to determine how the characteristics of the source RC pixel (and its PPRS neighbour) could be extrapolated from ID imaging (4-channel 64x2048 strip readout with 0.3406 s integration time) to predict how the same pixel would behave in Track (single channel 32x32 readout with 0.02508 s integration time) or Fine Guide (single channel 8x8 readout with 0.054168 s integration time) modes. Recall that the only time the complete array is obtained for the Guiders is by stacking ID image strips. There is no opportunity to collect a composite of the entire detector array using the 32x32 or 8x8 Track and FG readouts.

A proposed solution was to utilize the Double Asteroid Redirection Test Mission (DART) Moving Target observations to collect Track mode images in order to obtain a representative sampling of RC and PPRS pixels which could then be compared back to how those same pixels behaved in longer ID mode integrations. The advantage of using the DART data was that due to the higher motion rates, larger swaths of each Guider detector were covered during several passes of the observations. Figure 10 shows the Guide Star tracks across the detector grid from the DART observations. Figure 11 illustrates with 3 Track image frames the motion of the Guide Star as Track mode proceeds, with new bad pixels moving into the view as the window location changes. The counts of any imaged RC+PPRS pixels were extracted from this data and compiled into a representative sampling of behaviours for each Guider.

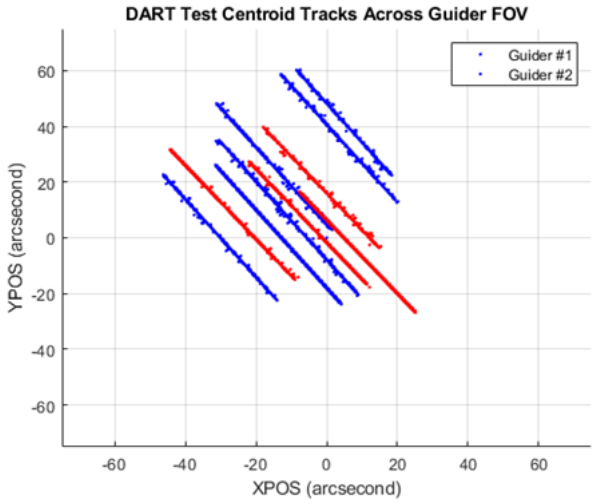

Figure 10: Guide Star locations in Track Mode During DART Moving Target Observations

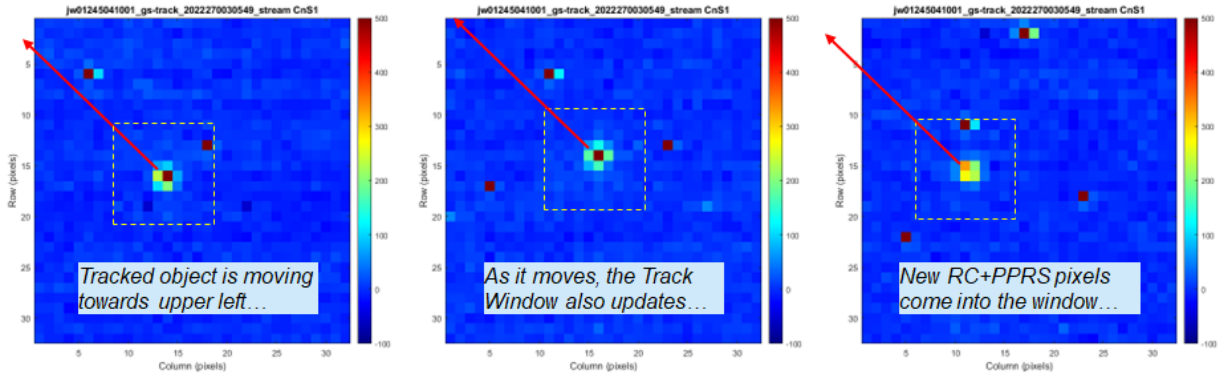

Figure 11: Three Sample Frames as Track Window Location moves across Guider 1 detector during DART Moving Target Observation (note the red arrow indicates the direction of motion of the Guide Star across the field of view)

From the compiled DART Track mode image data, plots of the PPRS neighbour pixel counts were plotted against the counts of the central RC pixel in order to determine the "PPRS%" as a general predictive rule. Figure 12 shows the results for Guider 1, with the Track mode PPRS% demonstrating a consistent slope of about 2.45%. Plotting the ratio for the same pixels from ID Mode imaging however shows a significantly lower PPRS% with a slope of 1.13%. This helps to explain why PPRS pixels were missed in the bad pixel mapping process when using ID mode images as the source data; the PPRS effect is actually significantly higher in the smaller subarray readouts.

Another interesting conclusion of the analysis was that the PPRS effect is dramatically lower for Guider 2 than for Guider 1. This is consistent with the observed failures, which happened exclusively when guiding on dim Guide Stars on Guider 1, and did not happen on Guider 2. The PPRS% for Guider 2 as shown in Figure 13 is on the order of 0.6%, and is more nearly consistent between ID and Track imaging.

The reason for the difference between Guider 1 and Guider 2 was traced back to differences in the bias tunings of the two detectors. It was determined during ground based tuning efforts that a trade-off could be made between different performance characteristics, with one outcome being that the tuning regime for Guider 1 was known to produce a higher PPRS effect, while the different tuning regime for Guider 2 was selected to minimize PPRS.

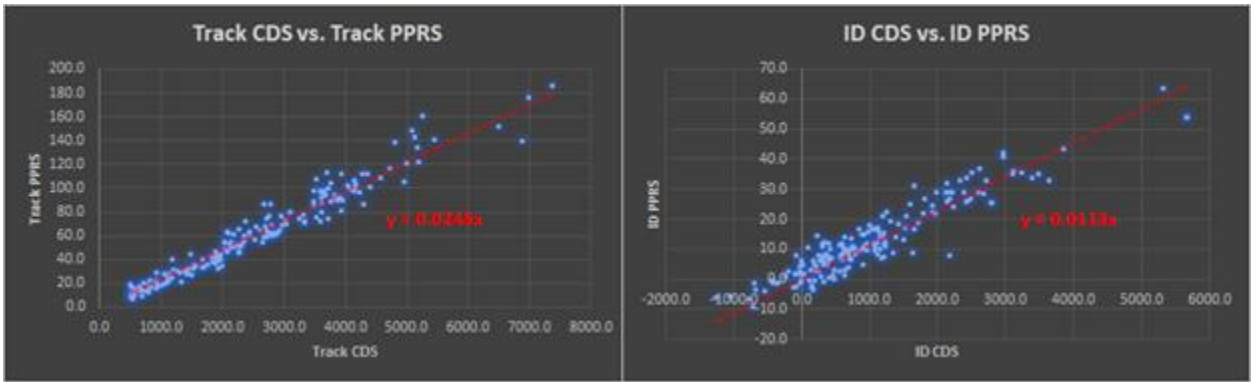

Figure 12: Guider 1 PPRS%: The slope of the PPRS vs. RC pixel counts in Track Mode (left) is 2.45% and ID Mode (right) is 1.13% for the same sample of pixels

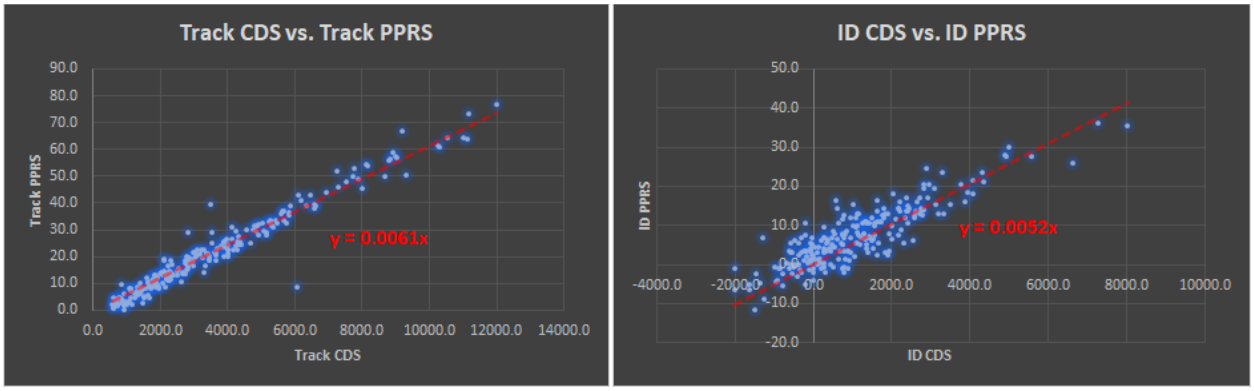

Figure 13: Guider 2 PPRS%: The slope of the PPRS vs. RC pixel counts in Track Mode (left) is 0.61% and ID Mode (right) is 0.52% for the same sample of pixels

Armed with this knowledge, the Bad Pixel Maps were revised using strictly on-orbit data. This resulted in "New Baseline" BPMs uploaded on orbit with "Rev 78" in early 2024, with the following modifications:

1. All RTN pixels were removed from the BPMs as the vast majority of these produce amplitude variations lower than 75 counts, which is a rough threshold for the lowest counts of a dim Guide Star peak pixel. With RTNs removed, occasional observations of a higher amplitude RTN pixel temporarily pulling the Track centroid away from dim Guide Stars have subsequently occurred. But since these RTN pixels only periodically jump to the higher count, the window does not stay centered on the RTN pixel and returns to the Guide Star peak pixel. This has nevertheless occasionally produced an error if the RTN pixel jump occurs right near the end of a Track mode operation and the FGS FSW is using that location to extrapolate the position for placing the Fine Guide window. While we do not yet have statistics for the occurrence of this offset error, it is a rare event. This issue may be addressed in future FSW patches.
2. All PPRS pixels were removed from the Guider 2 Bad Pixel Map. Moving forward, PPRS pixels could be added back if they pass set thresholds when evaluating the ID image data for new updates, however they are not added unless they do (since ID and Track mode PPRS levels are deemed to be essentially equivalent between ID and Track/FG mode imaging for Guider 2). This significantly reduced the overall population of bad pixels in the Guider 2 BPM, as it was unnecessarily carrying many PPRS pixels in the original baseline.
3. For Guider 1, a process was developed where PPRS pixels would automatically be added for the brightest (or "fastest") RC pixels found in ID mode imaging, independent of whether they passed set threshold levels or not. This is because of the higher PPRS% in Track/FG imaging modes for Guider 1, and the general

inability to predict RC pixel levels at shorter integration times. For the "slower" RC pixels, PPRS neighbours might or might not be added, depending on whether they passed the ID imaging threshold levels or not.

With these modifications, at the time of writing this paper with "Rev 95", the Guider 1 BPM contained 11503 bad pixels (0.287%), and the Guider 2 BPM contained 13727 (0.343%). Now that the classification and counting methodology for on orbit operations has been stabilized, it is anticipated that the populations will continue to demonstrate the steady growth rate observed to date due to approximately steady radiation flux at the JWST orbit. Figure 14 shows the incremental growth in Guider 1 and Guider 2 bad pixel populations for several ~monthly revisions of the BPMs in the second and third years of normal operations.

Note that if the bad pixel populations continue to grow by ~40 pixels per month, per detector, then over 10 years the total populations would only grow by 4800 pixels per detector. At this rate, the bad pixel populations would remain under 0.5% of the total active pixel area, and would not result in any significant impact to Guider performance. It is not known if any additional detector aging effects might eventually cause the rate to increase over time.

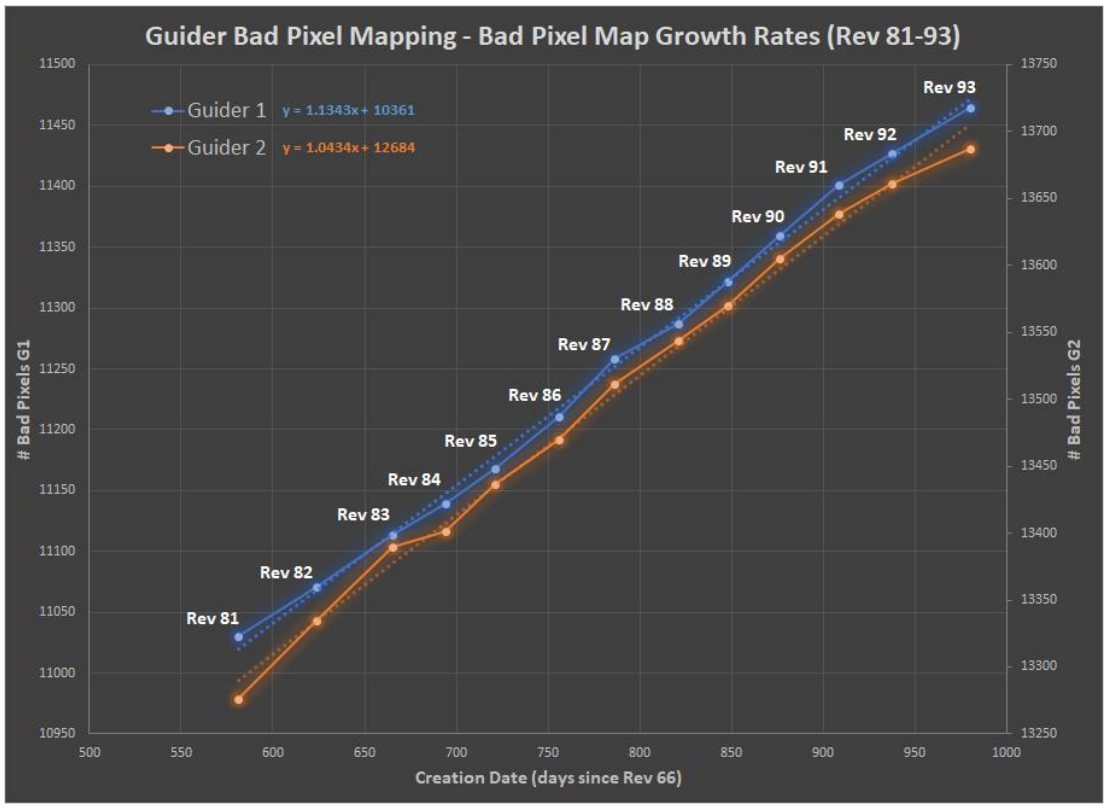

Figure 14: FGS New Baseline Bad Pixel Map Growth Rate during Normal Operations

4. Guide Star Catalog and FGS Commanding

Several optimizations to how Guide Stars were selected from the Guide Star Catalog (GSC) for FGS commanding arose during the course of Commissioning. It became apparent that the photometric conversion gain used to predict instrumental counts based on star catalog magnitudes was too low on Guider 2. A correction factor of 1.25 was determined empirically by comparing observed Guide Star amplitudes to catalog predictions. This correction factor was applied to the initial Guider 2 gain value on May 12, 2022 and has remained in use subsequently. Note that

Guider 1 did not require any such correction. The DART moving target test provided a useful check of multiple Guide Stars within the same visit, demonstrating good correlation between the star catalog (commanded) count rates and magnitudes and those observed with both FGS Guider 1 and Guider 2, as illustrated in Figure 15 [6].

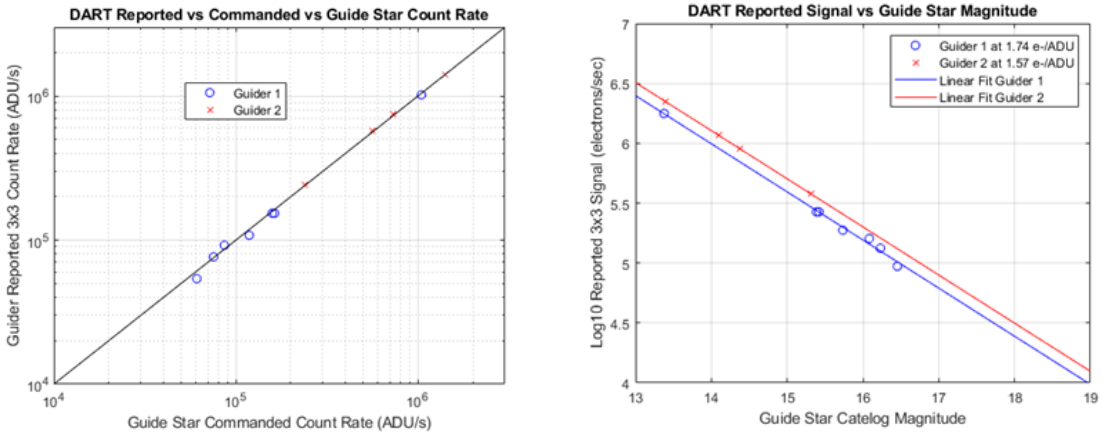

Figure 15: Reported Guide Star Count Rate vs. Command (left) and Reported Guide Star Intensity vs Expected Guide Star Catalog Magnitude (right) for Observations During DART Mission

The origin of this discrepancy in the pre-flight estimates of the guider sensitivity is currently believed to be in the method used to interpolate the complete detector response (quantum efficiency) vs wavelength from the limited QE vs wavelength data obtained during the Guider detector characterization. The quantum efficiency at wavelengths below 1.5 µm, where more than 70% of the guide star intensity resides, is determined primarily by two detector characteristics, the anti-reflection coating applied to the detector material and the quantum yield of the material. Since the energy of photons > 1.5 µm is significantly greater than the detector bandgap, there is the statistical probability of more than one photon electron being generated in the material at these wavelengths, this is the quantum yield. Since the response of the FGS detectors was only determined at wavelengths of 0.8, 1.23, 2.0, 3.5 and 4.4 µm, an interpolation had to be used to provide an overall detector response function for any wavelength which could then be convolved with the spectral energy distributions for typical guide stars. A similar method was used to interpolate the guider optical throughput from measured optical component data. However, the detector anti-reflection coating has structure below 1.5 µm (see Rauscher et al [7]). For the NIRSpec detectors in that study the response below 1.5 µm was relatively consistent and it was assumed that this should hold true for the Guider detectors, but apparently this was not the case. In particular, the Guider 2 detector has a better performing AR coating at short wavelengths at the 10-15% level and this is in turn amplified by the quantum yield. This resulted in Guider 2 being 25% more responsive than Guider 1 to typical guide star spectral energy distributions.

Several other optimizations were implemented over the course of Commissioning and normal operations related to commanding FGS. These were applied at the GSC or Guide Star Selection System (GSSS) level, or involved checks or parameters passed through the Operations Script Subsystem (OSS).

- Guide and Reference stars are chosen from the GSC and passed to FGS via OSS. With each commanded star, a tolerance threshold is supplied along with the expected star amplitude so that FGS FSW can check if an identified star falls within the expected range. At launch, this tolerance was originally set to be +/- 30% of the expected Star amplitude. However, it was determined during Commissioning that due to a combination of GSC photometric uncertainty and occasional high detector photo-response non-uniformity (particularly for Guider 1 – see Section 7 of this paper) the threshold needed to be raised to 35%. Subsequently in December 2024, the tolerance was raised again to 40%.

- The overall allowed magnitude ranges for choosing Guide and Reference Stars from the GSC was refined based on operational experience. The current GSSS ranges are: for Reference Stars the magnitude range is J= 10.0-18.0 (allowing very bright Reference Stars, which is particularly useful in Bright Crowded Fields) and for Guide Stars the range is J= 12.5-18.0.

- A special case for the GSSS allowable magnitude range was defined for Moving Target observations. In these cases, the Guide Star energy may be spread across more pixels than usual due to the motion rate. After Commissioning, the lower Guide Star allowable magnitude was increased to J=16.5 (G1) and J=17.0 (G2) which gives ~ 55,000 ADU counts/s on the FGS 3x3 pixel window.

- Normally, for efficiency, the GSSS commands a Guide Star for the ID process to be at the same position it will be needed in for the science observations (its "science position"), with the exception of Bright Crowded Fields and Moving Target visits, where the Guide Star is commanded to the center of the detector for ID. Due to the potential for initial ACS pointing errors coming out of the Observatory slew to new pointings, a decision was made to ensure that the GSSS would not command a Guide Star to be less than 15" from the edge of the FGS detector field of view for the ID process, but would still command the GS to be as close as possible to its science position. However, Guide Stars can be commanded to science positions as close as 71 pixels from the edge of the detector.

- It has been an ongoing exercise to update the GSC to ensure that galaxies (or other non-stellar objects, e.g. star clusters) should not be used as Guide or Reference Stars. Prior to JWST launch, other sky surveys have not always been able to distinguish between these types of entries in the original GSC input sources. However, any such misclassified objects can appear as extended objects in the sensitive JWST images. For FGS, this can spread the energy of the object across more pixels than would be expected for more point-like stellar sources, and result in lower-than-expected count rates within the 3x3 pixel amplitude counting area used by FGS. In such cases, these extended objects often fail subsequent amplitude checks. It is an ongoing process during JWST operations to flag any instances of this occurring and to update the GSC accordingly to exclude these types of extended sources.

- The GSSS also implements an exclusion zone to ensure that a Guide Star is selected which has no other stars within 2 magnitudes of brightness within 6" of separation from it. This helps to avoid potential errors within the Acquisition mode window, particularly after a slew from identification to a science pointing. The high JWST resolution has also yielded increased knowledge about binary and other multiple star systems, and the GSC continues to be updated to reflect cases where an original catalog star entry may turn out to have one or more nearby companions (either real or optical).

See also Section 8 of this paper for updates made to the GSC to incorporate improvements for use in Bright Crowded Fields (e.g. galactic center observations). GSC 3.1 was implemented for FGS commanding in December, 2024.

5. Detector Saturation

The FGS detector readout converts pixel signal values into a 16-bit digital number. Therefore, the maximum digital pixel value is nominally 65,535 ADU. However, the effective dynamic range for integrating signal on a detector pixel is necessarily lower than this digital limit. The detector biasing has been tuned to ensure a bias offset several thousand ADU above zero, and each pixel has its own slightly different offset, gain, and therefore effective dynamic range.

In the Guider operational modes, variable offset is accounted for with differenced image schemes, typically correlated double sampling (CDS) in most modes, with an initial pedestal image readout subtracted from a later signal image readout while integration proceeds. The FGS flight software also provides the option for effectively

correcting gain for each pixel as part of its Photo-Response Non-Uniformity (PRNU) table (although as noted in Section 7, this correction has been disabled throughout JWST operations). But no allowance has been made for a variable "upper limit" or pixel saturation count on a pixel-by-pixel basis. Instead, FGS flight software in the two modes where saturation is most likely to occur (ID and ACQ1 – the two modes with the longest integration time) has defined a single fixed parameter "*rawSatPixelLimit*" in a configuration data table which is intended to be used for all pixels across the detector. Prior to launch the value of this parameter was set based on fully saturated full-frame readouts collected during ground flat field imaging tests. Histograms of the saturation points for every pixel were generated, as shown in Figure 16.

For Guider 1 most pixels saturated somewhere between 55,000 and 64,000 ADU counts. Guider 2 had a similar but slightly wider range, saturating from about 53,000 up to 65,000 ADU counts. Prior to launch, the decision had been made to inset the "*rawSatPixelLimit*" parameter slightly inset from the leading edge of these histograms, by setting it to 57,000 ADU for Guider 1 and to 56,000 ADU for Guider 2, as a compromise to account for the fact that the single value would be used for all pixels on each detector.

Any time a pixel registers a value above the saturated pixel limit in ID or ACQ1 modes, its CDS value is replaced by a parameterized fixed value of 25,000 counts. This helps to maintain a standard minimum count rate for bright stars, since a bright star with one or more saturated pixels might otherwise show a diminished or even zero signal if saturation occurred in the pedestal image prior to CDS differencing.

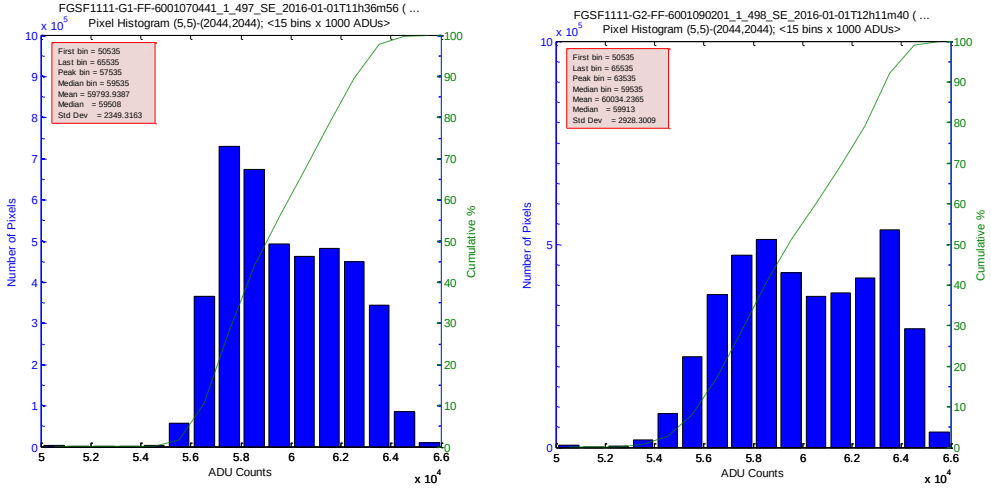

Figure 16: Guider 1 (left) and Guider 2 (right) Pixel Saturation Counts from Ground Testing

In practice, however, during Commissioning, it was found that many pixels saturated at lower counts than the "*rawSatPixelLimit*" settings. This meant that inaccurate star count rates were frequently generated in ID mode in particular. Guider modes require star amplitudes to fall within a set threshold of the expected value, and due to some saturated pixels failing to reach the "*rawSatPixelLimit*" setting, they were differencing to very low count rates and causing selected Guide Stars to fail their amplitude checks.

This resulted in an effort to revisit the "*rawSatPixelLimit*" settings during early Commissioning. Because it was no longer possible on orbit to completely saturate the entire detector readout with a flat-field illumination source, the approach taken was to generate a "conglomerate" image from many visits (once the detector temperature had stabilized around 39.5K), stacking as many bright and saturated stars (or other celestial objects) as possible into a single display. For Guider 1, a total of 278 separate image frames were stacked to try to gain the most representative possible sampling of saturated pixels across the detector. Figure 17 shows the resultant stacked image for Guider 1, along with a histogram of the resultant image counts.

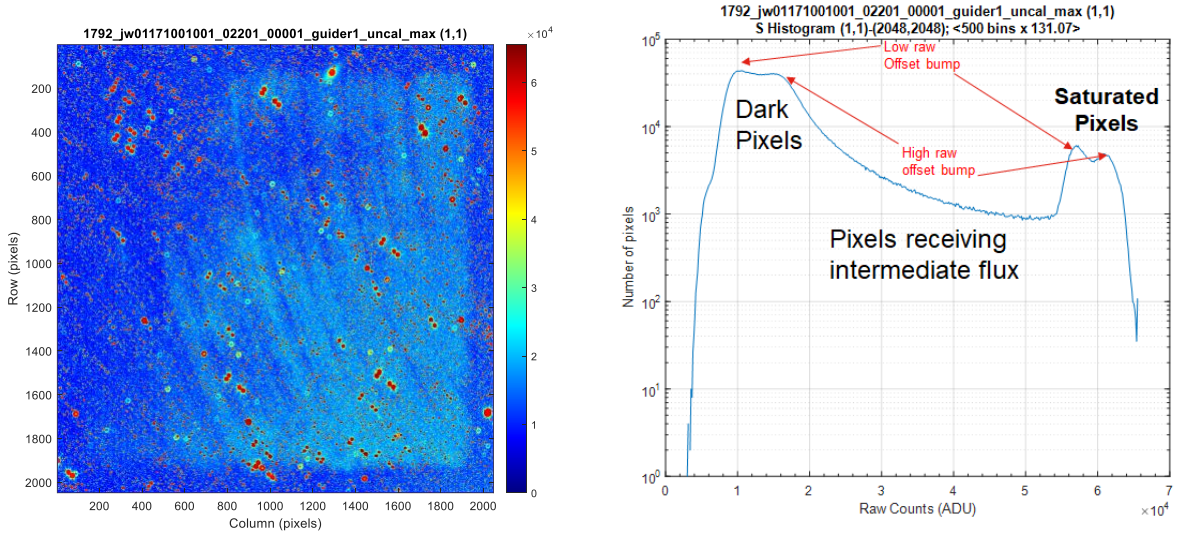

Figure 17: Guider 1 Conglomerate Bright Image (left) and Pixel Count Histogram (right)

From this conglomerate image, the subset of saturated pixels was examined to determine a better choice for the "*rawSatPixelLimit*" parameter setting. It was noted that the necessary approach to choosing the value was to set it at the "onset" of the saturated pixel histogram, as a "worst case", since it was going to apply to all pixels on the detector, and a Guide Star could land on any pixels. A similar approach was followed for Guider 2.

In the end, it was determined that the best "onset" saturation values to set were 54,500 ADU for Guider 1, and 53,000 ADU for Guider 2, as illustrated by the saturated pixel tail histograms of Figure 18. These settings have been maintained throughout the course of JWST normal operations and have proven to be satisfactory selections to optimize Guider performance.

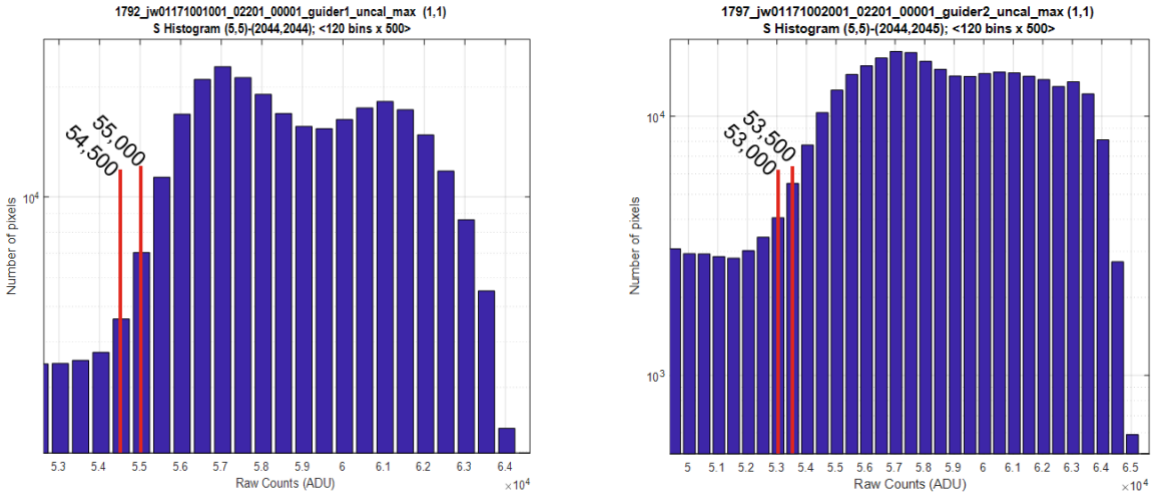

Figure 18: Saturated Pixel Histogram Tails for Guider 1 (left) and Guider 2 (right)

6. Other Guider FSW Data Table Parameter Updates

Several variables related to the FGS flight software (FSW) algorithms which are executed during Guider operational modes are parameterized into a series of mode-specific data tables. This was done as part of the FGS FSW design in order to allow the parameterized values to be updated if needed on-orbit when more operational experience was obtained, through data table uploads, without needing to modify the overall FSW source code.

Over the course of JWST Commissioning and early operations, several parameters were updated in order to optimize Guider performance. Table 2 provides a list of these updated parameters (along with a couple FSW code changes), and a brief description of the rationale for updating them. The impact of the updates is summarized here.

Table 2: Summary of FGS FSW Data Table Parameter and FSW Code Updates

Execution Date	Applicable Modes	Parameter	Update	Comment
28-04-22	ID / ACQ1	rawSatPixelLimit	G1= 54500 G2= 53000	See Section 5
13-05-22	All	Distortion Tables	Distortion coefficients data table	See Section 2
26-05-22	ACQ1	AbsMatchError	From 54.8 to 60 pixels	To allow for more ACS initial pointing error when executing a Medium Angle Maneuver
30-10-24	ACQ2	DeltaSignalThreshold	From 6 to 8	Effectively disable this centroid quality check during ACQ2
30-10-24	ACQ2	DeltaNoiseThreshold	From 6 to 8	Effectively disable this centroid quality check during ACQ2
30-03-23	ID	Epsilon	From 132000 to 72000	Better triad match performance on orbit than worst-case ground analysis allowance
30-03-23	ID	AttitudeError	From 14.5 to 2	Better ACS pointing accuracy in Roll than worst-case ground analysis allowance
30-03-23	ID	AbsMatchError	From 562.5 to 220	Better ACS pointing accuracy in X-Y than worst-case ground analysis allowance
01-09-22	ID / ACQ 1	MergeIntensiyPercent	From 0.8 to 0.7	Larger variation in Guide Star counts between successive integrations than predicted
01-09-22	Track	subWinUpdateCriteria	From 2 to 4 pixels	Allows for ability to execute Moving Target observations at higher motion rates
19-01-23	Track	FSW Patch	FSW code updates	16-bit Integration count number rollover for long Track mode observations and clearing of bad pixel correction data
12-03-25	ID / ACQ1	FSW Patch	FSW code updates	To improve performance in Bright Crowded Fields

ACQ2 *DeltaSignalThreshold* / *DeltaNoiseThreshold* parameters

DeltaSignal and *DeltaNoise* are Guider centroid quality indicators calculated based on the variation of the computed Guide Star centroid signal and noise. If the measured signal or noise change between integrations beyond certain limits, it suggests that perhaps something has occurred to degrade the centroid observation. This can happen for example when a Guide Star traverses a bad pixel on the detector, or is affected by a cosmic ray or some other external source which injects uncertainty into the computed Guide Star centroid. The values of *DeltaSignal* and *DeltaNoise* are scaled onto just 3-bit quality indicators in the centroid data packet (i.e. integer values from 0-7).

Both of these values are most important during Guider Track and Fine Guider operations, when numerous integrations of the Guide Star are performed in small subarray readouts. Nevertheless, the values are also calculated for the ACQ2 mode as well, which serves as a bridging readout from ID and ACQ modes to the Track mode. However, only 5 exposures are taken in ACQ2 mode, and the algorithm requires successful confirmation of the Guide Star in 4 out of 5 of these exposures. Any instance of a *DeltaSignal* or *DeltaNoise* calculation exceeding the threshold setting marks the centroid as "bad", and results in a non-successful exposure. This is useful in Track and Fine Guide when there are many exposures, and any potentially erroneous centroids may be marked bad and removed from the ACS solution, without negatively impacting the overall successful continuation of the Guider operation mode.

However, in ACQ2, it was encountered that in practice, due to various factors, there was some possibility of excess post-slew drift of the Guide Star onto pixels with varying photosensitivity, or which otherwise result in *DeltaSignal* or *DeltaNoise* values which resulted in "bad" centroid indications. These occasionally caused Visits to fail due to not achieving 4-out-of-5 successful ACQ2 exposures.

It was decided that the evaluation of these centroid quality indicators was not necessary for the ACQ2 mode. They are only relevant to the many-exposure scenarios in Track and FG modes. Therefore, by increasing the values *of DeltaSignalThreshold* and *DeltaNoiseThreshold* in the data parameter tables for ACQ2 from 6 to 8, the evaluation is effectively disabled – because on a 3-bit scale, the maximum value which can be computed is 7. Setting the thresholds to 8 therefore effectively removes the possibility of these quality indicators generating a bad centroid in ACQ2.

ACQ1 *AbsMatchError* parameter

This parameter sets the threshold for the difference in the absolute position between the expected position of the Guide Star on the Guider detector, and the location at which it is deemed to be found during Acquisition mode (in pixels). Based on a buildup of estimated potential positional errors for the Guide Star when transitioning to ACQ1 mode from ID mode, the original value of the *AbsMatchError* had been set to 41.3 pixels prior to JWST launch.

However, in practice it was found that sometimes a large residual ACS drift after the slew from the identification pointing to the science pointing could result in the Guide Star landing further from the center of the 128x128 ACQ1 imaging window than anticipated. The value of the *AbsMatchError* parameter was increased to 54.8 pixels and then to 60.0 pixels during Commissioning in order to give the best chance of finding the Guide Star if it happened to land anywhere within the 128x128 ACQ1 imaging window.

Figure 19 illustrates the difference between allowing a Guide Star to land within 41.3 pixels of the center of the 128x128 ACQ1 imaging window (dashed line) and within 60.0 pixels (solid line).

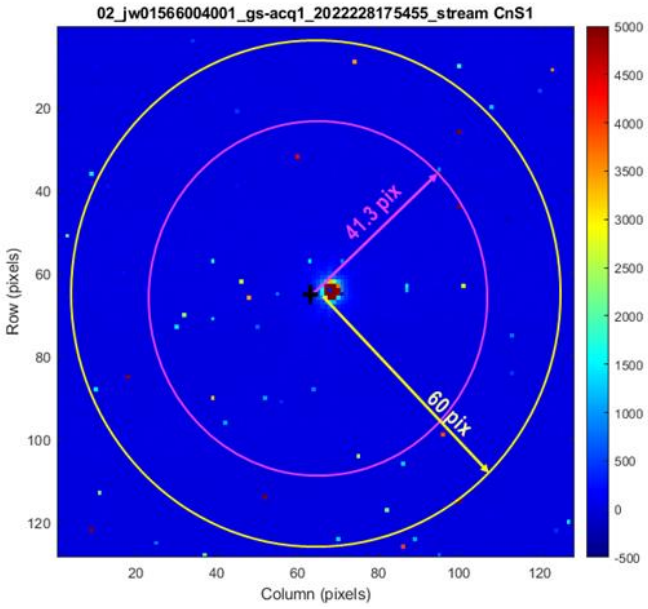

Figure 19: Difference between *AbsMatchError* 41.3 pixels and 60.0 pixels in ACQ1 128x128 image window

ID Mode: *Epsilon, Attitude, AbsMatchError* parameters

There are several parameters associated with the error tolerance on matching star triads to identify a candidate Guide Star in ID mode. Of these, three parameters were refined after considerable analysis of the on-orbit ID mode performance in the first year of normal operations. The *Epsilon* parameter is based on a series of factors associated with the triad "shape" – combining star separations and internally subtended angles. Ground simulation with worst-case analyses suggested a value of 132,000 for this parameter. Subsequently on orbit, it was found after examining many ID mode cases, and re-simulating these visits with lower *Epsilon* settings, that a value of 72,000 could improve results. This helps to reject excess poor triad match candidates during the matching process, and to ultimately result more frequently in the correct solution.

Similarly, the parameter *AttitudeError* was reduced to improve the ID performance. This parameter is essentially a tolerance on the allowed "roll" error of a candidate triad solution relative to the commanded celestial catalog positions of Guide and Reference stars. During normal operations, it was noted that the Observatory ACS pointing typically achieves the commanded roll angle to well within an arcminute. However the pitch/yaw drift of the Observatory during the imaging of the ID strips can cause a triad to appear to have undergone rotation. Reducing the allowed roll angle error for candidate star triad solutions from 14.5 degrees to just 2.0 degrees was found to better include the intended target triads while excluding others, providing a significant performance improvement especially in crowded field scenarios.

Finally, the *AbsMatchError* component of the ID algorithm was reduced from 562.5 to just 220 pixels. This is an absolute position check of located star positions vs. their expected positions considering the star catalog and intended Observatory pointing. It was set very large (at least in terms of Guider pixels) to accommodate large potential Observatory ACS pointing offsets. However, in practice on orbit, it was found that the majority of post-slew pointings would normally be within 10" of the targeted pointing (~142 pixels). This 10" value was ultimately implemented as an upper limiting threshold on the final Guide Star location by OSS; any identified Guide Star falling more than 10" outside of its expected location would constitute a failure at the OSS level and require a Guider ID

mode re-try. At the same time, within the FGS ID FSW algorithm, any star (guide or reference) which fell outside the *AbsMatchError* threshold of a commanded star would be excluded from the candidate solutions. It was determined that narrowing this threshold from the initial very high value helped to eliminate unnecessary "similar triad" solutions.

In early 2023, a series of parameter sensitivity simulations were executed using image data downloaded from on-orbit Visits. Repeated execution of these test cases with varying values of *Epsilon, AttitudeError*, and *AbsMatchError* resulted in the selected reduced values in order to optimize Guider performance in ID mode.

ID/ACQ1 *MergeIntensiyPercent* parameter

Note the spelling here is per the actual parameter name. This parameter dictates the allowed tolerance between candidate Guide Star amplitude values (3x3 pixel count rates) across the 2 integrations performed in ID and ACQ1 mode for each attempt. The original value at launch was 0.8 (or 80%). That is, the expected count rates for a given candidate Guide Star should match within 80% between the two reads in a given ID or ACQ1 attempt, in order for the candidate to be considered. This parameter was set to allow for some possible readout variations as the star drifted onto pixels with different photosensitivity, or was pixelated differently across the detector grid during reads. However, in practice, it was found that due to a higher than anticipated variation in intensity across different pixels (especially on Guider 1), the performance could be improved by reducing this match criterion to 0.7 (or 70%).

Track Mode *SubWinUpdateCriteria* parameter

In FGS Track mode operation, the location of the 32x32 subarray which is read from the detector is constantly updated in order to attempt to keep the Guide Star centered in the window. The *SubWinUpdateCriteria* parameter controls how much of a change in the calculated Guide Star centroid location, in pixels, is required in order to trigger a new subarray readout location. During many science observations, the subarray window readout location ideally remains static, or moves only slightly in conjunction with the ACS Fine Steering Mirror for small dithers. However, it was found that in order to accommodate Moving Target visits, particularly at higher motion rates, it was necessary to trigger this update to occur for larger movements. Moving Target visits involve observations of solar system objects such as asteroids or other planetary bodies.

After a window move, the first 3-4 centroids are marked bad to allow for overall system latency. Allowing FGS FSW to reliably calculate a centroid location based on the updated window location. ACS does not use FGS centroids marked bad. The rate of occurrence of this sequence of bad centroids will depend on the commanded moving target rate and the *SubWinUpdateCriteria* parameter. Initially this was set to be 2 pixels, however, when faster moving targets were considered this parameter was updated to 4 pixels to reduce the rate of bad centroid occurrences due to window moves that might impact the FSM control loop. The original FGS requirement was to be able to track objects moving in the FOV at up to 30 mas/s. It was found that this could be extended above 70 mas/s with the updated parameter. In practice, during the Double Asteroid Redirection Test observation, rates of up to 110 mas/s were achieved.

Track Mode FSW Patch

Improving FGS performance via updates to data table parameters has been the preferred method wherever possible. Where this is not possible, a patch to the FSW code may be uploaded to the Observatory instead. Generating these code patches requires a far greater effort in terms of ground validation. Very few actual "bugs" in the FGS code have been discovered during the course of JWST Commissioning and Normal Operations. Recently, as described in Section 8, an update to FGS ID and ACQ1 mode image processing software was made in order to improve performance when operating in Bright Crowded Fields (BCF). This was an optimization, but not a bug fix. However, a pair of actual bugs

were discovered in the way the FGS FSW behaved during extended Track mode activities. These bugs were fixed and uploaded as patches to the FGS FSW.

During most FGS activities, the goal is to enter into a long duration Fine Guide mode, and only briefly pass through Track mode, taking only on the order of hundreds of Track mode integrations. But during a Moving Target visit, FGS remains continuously in Track mode. For a slower moving target, this may result in many thousands of successive integrations in Track mode before an object passes outside of the JWST field of view. It was discovered that two issues could arise whenever a 16-bit count of the number of integrations reached its maximum value of 65,536 and then rolled over to begin counting at 1 again. Track observations with that many integrations had never been simulated on ground before, so the bugs remained undetected until encountered during a very slow-moving target Visit during normal operations. When the counter rolled over, centroids were marked bad, and a flag for marking pixel correction data was not cleared when exiting Track mode. The FSW patch to accommodate this rollover was successfully implemented on orbit, helping to provide growing confidence to the FGS FSW team in its ability to continue to apply such patches to address any future bug fixes to further optimize FGS performance, for example as described in Section 8 for BCF observations.

7. Photo-Response Non-Uniformity (PRNU) and Countrate Variation

Every pixel on the FGS detectors has a unique response to incident light. These responses are bounded within a relatively narrow regime of normal behaviour for the vast majority of pixels. Nevertheless, every pixel does indeed demonstrate an individual "photo-response" or "gain" relative to incident photons. This was understood in early instrument design, and the FGS flight software was designed to accommodate for a pixel gain correction table which could be optionally enabled or disabled via FSW parameter in order to correct for this effect on a pixel-by-pixel basis.

Calibrating this correction table has proven to be very challenging in practice. During ground-based cryogenic testing[8][9][10], full-frame flat-field illumination testing was used to develop the baseline Photo-Response Non-Uniformity (PRNU) correction data tables. The overall photo-response showed very different characteristics on the Guider 1 and Guider 2 detectors. Due to manufacturing differences, the Guider 1 detector had a significantly larger PRNU variance than the Guider 2 detector. This can be seen in the PRNU correction value histograms of Figure 20.

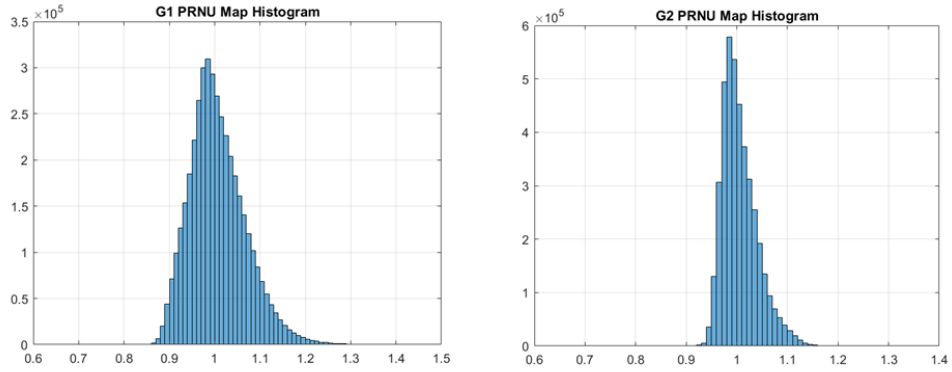

Figure 20: PRNU Correction Factor Histograms for Guider 1 (left) and Guider 2 (right) based on Ground Testing

Additionally, it has been observed that the illumination methodology applied during ground-based testing does not match well with results from on-orbit observations. The method of flat-field illumination applied during ground tests appears to produce a significantly different pixel photo-response relative to on-orbit observations when point-source illumination (stars) is observed. This is believed to be an effect of how the incident illumination registers on

the detector crystal lattice, which is different for a flat-field source than it is for point-source illumination from stars. The effect is significantly amplified on Guider 1, which is known to have a distinct "cross-hatching" pattern visible from its manufacturing process relative to Guider 2. Figure 21 illustrates PRNU correction tables for the two Guiders. Guider 1 (left) has a distinct "cross-hatching" pattern, while Guider 2 is overall "smoother" (albeit with a distinct non-uniformity outline in the upper-center believed to be caused by a "bubble" in the detector layer adhesive). The standard deviation of corresponding PRNU correction values is inset in a histogram, illustrating the very different characteristic PRNU behaviour between Guider 1 and Guider 2.

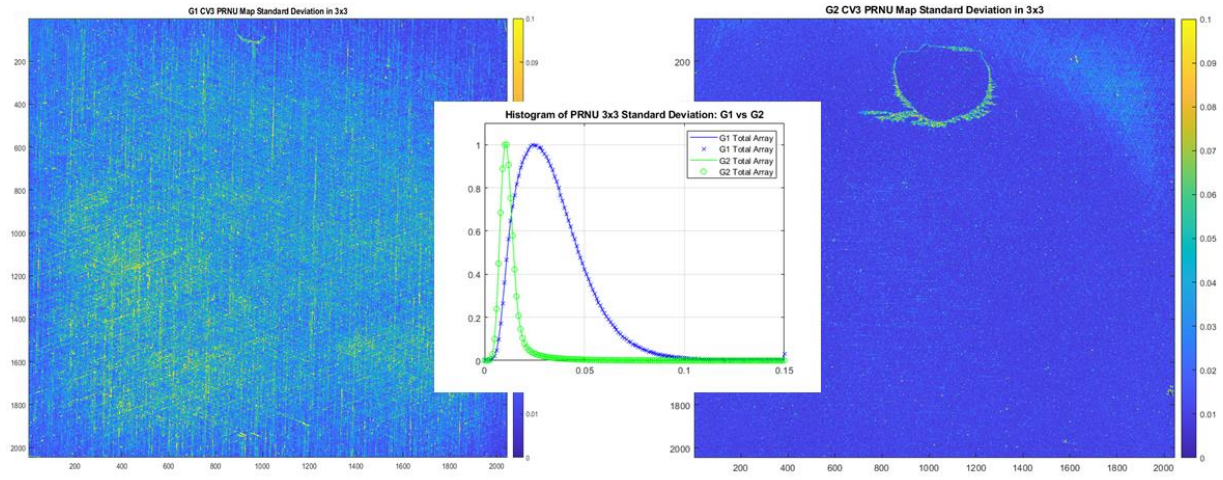

Figure 21: Guider 1 PRNU (left) vs. Guider 2 PRNU (right) with comparative standard deviation histogram (inset)

Due to the uncertainty carried forward about the efficacity of ground-based PRNU correction data tables, FGS flight software was programmed prior to launch to disable the PRNU correction entirely for both guiders. It was deemed unlikely that Guider 2 would require any correction at all. For Guider 1, while an accurate correction might enhance performance, none of the ground-based testing seemed to promise an effective means of correction. A correction table was uploaded for Guider 1 based on ground test results, but disabled in application, while a "flat" correction table was uploaded for Guider 2, and also disabled.

The PRNU effect has nevertheless had an occasional significant impact on Guider operations on orbit. An anomaly occurred during Commissioning due to centroid offsets and Guide Star amplitude failures introduced by the effect of PRNU variations on imaged Guide Stars. This was first observed during Moving Target observations when a target Guide Star transitioned across regions of Guider 1 with significantly different PRNU, resulting in centroid offset variations and amplitude variations as the moving target source traversed different pixel locations on Guider 1. In general, whenever an imaged Guide Star lands on a detector region with significant PRNU change, the measured Guide Star count rate may drop below the threshold applied to the expected count rate, resulting in a Guide Star amplitude check failure.

This effect was illustrated repeatedly in early Guider operations. In Figure 22, a targeted star was imaged repeatedly on both Guiders with small angle dithers performed between imaging sequences. Initially on Guider 1 in Observation 4, it registered a variable count sum, although it was imaged at a detector location which had minimal PRNU variation. Subsequently in Observation 5 it was imaged on Guider 2, with very low PRNU variation. Then it was imaged again on Guider 1 in Observation 6 in a detector region which produced very significant variation between dithers. This magnitude of count variation can exceed the commanded Guide Star amplitude thresholds and cause an observation to fail.

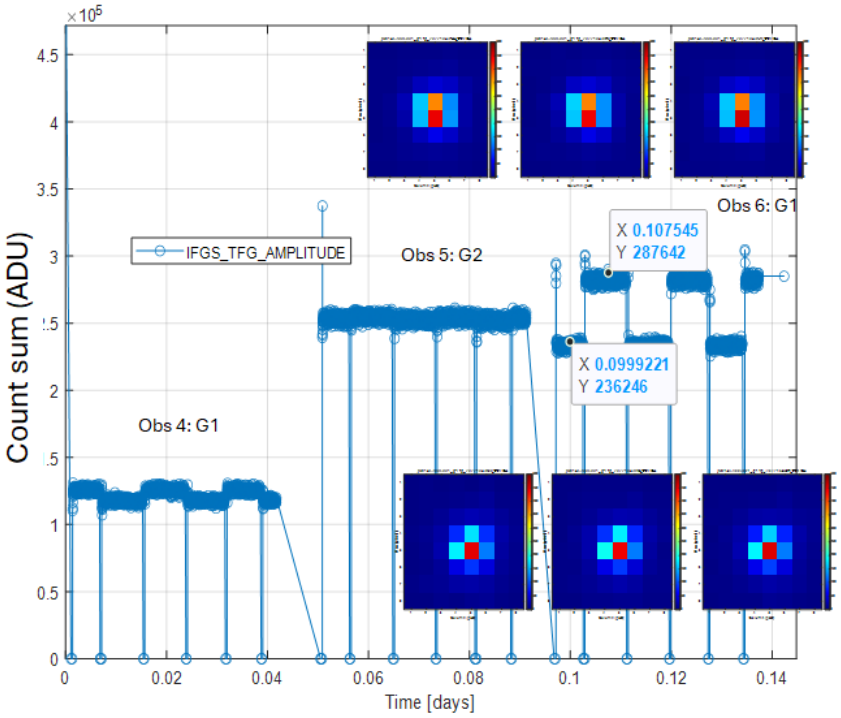

Figure 22: Illustration of Countrate Variation caused by PRNU; 6 dithers in Obs 4 on Guider 1 in moderate PRNU location, followed by 6 dithers in Obs 5 on Guider 2 with very low PRNU, followed by 6 dithers in Obs 6 on Guider 1 with very high countrate variation

Currently, the mitigation on-orbit for large PRNU variations on the Guider detectors has been to increase the commanded tolerance on Guide Star amplitude. From 30% at launch to 35% during Commissioning and recently to 40% (see Section 4 of this paper). This has the combined effect of helping to mitigate against PRNU variations on the Guider detectors, while at the same time mitigating against effects of photometric uncertainties in the Guide Star Catalog.

It remains an open question as to whether a refined PRNU map might be constructed based on operational image data which might offer a more effective mitigation against this effect. This would presumably be most valuable for Guider 1. Future analyses which pull in Guider 1 image data across many hundreds of operational Visits to date could be used to help construct an improved PRNU correction map which accounts for the realistic point source imaging effects of Guide Stars on the FGS detector. Enabling the PRNU correction could have some timing implications for FGS FSW in Track and Fine Guide, so any decision to do so will require testing. An alternative option is to better account for low photo-responsivity pixels in the existing Bad Pixel Maps.

8. Center of the Galaxy and Bright Crowded Field (BCF) Operations

FGS operations in Bright Crowded Fields (BCF) such as near the Galactic Center (Sgr A*) have represented another significant on-orbit challenge. In this region of the sky, there is such a heavy concentration of stars at the brighter end of the FGS sensitivity range that the Guider Identification (ID) mode was frequently failing to find the commanded Guide Star. In some cases, it would fail out of ID mode entirely and science Visits would be skipped. In other cases, it would misidentify the Guide Star, and then fail in subsequent modes as the image integration time was reduced and the full star amplitude became evident resulting in failed brightness checks against the star catalog.

In early normal operations it was estimated that only ~25% of BCF visits resulted in identification of the correct commanded Guide Star.

It was already anticipated from ground simulation that a special readout approach would be required for this region of the sky. Normally in ID mode, the Guider detector is read out in a series of slightly overlapping 64x2048 strips. Thirty-six of these strip images are required to cover the entire 2048x20248 detector (save for a small number of rows at the top and bottom). For most normal pointings in the sky, fewer than 100 "bright objects" (i.e. candidate Guide Stars) will be found within the Guider FOV and magnitude sensitivity range (J = 12.5 to 18.0). Typically the number is much lower than 100. Consequently, the FGS ID mode algorithm is designed to allow a maximum of 100 bright objects to enter the subsequent pattern matching stage for identification. The ID image area is scanned to create a "bright objects list", ordered by observed brightness, and confirmed by matching across 2 unique integrations (in order to remove any transient objects such as cosmic ray hits).

However, in BCF regions, there are many more than 100 such bright objects. Therefore, OSS commands a special readout mode for BCF fields such that only the central 12 strips of the FGS detectors are read out. The Guide Star and any Reference Stars to be used for pattern matching in ID are constrained by the Guide Star Selection System to fall within this central region of the field of view.

Nevertheless, even with this prior design accommodation, FGS performance in BCF fields was very poor during early normal operations, and significant effort was put into trying to determine ways to improve the performance.

One of the first findings in this investigation involved revising the Guide Star Catalog (GSC) for the Galactic Center region of the sky. Figure 23 helps to illustrate the issue discovered. The initial GSC at launch (version 2.4.3.1) only contained a sparse sampling of the visible stars in this region of the sky. Additionally, the position and photometric accuracy for many stars was very poor. The same region of the sky is shown in Figure 23 in 3 panels: the left is a simulated image constructed from the original GSC 2.4.3.1 at JWST launch, then center is the same location imaged by FGS, and the right is the same location simulated with data taken from an external Galactic Nucleus Catalog (GNC)[11] combined with data from Gaia ER3. The analysis also showed that the standard algorithm converting the GNC photometric J,H,K magnitudes to FGS counts underpredicted what FGS would see by a factor of 1.25 to 1.9 due to the extreme reddening of stars near the galactic center.

Therefore, it was determined that an update to the GSC to incorporate new information derived from the external star catalog sources was essential in order to be able to provide more accurate commanded Guide Star and Reference Star information as an input to the FGS ID process. An average scale factor of 1.5 was put in place to apply to the GS counts for visits on this area of the sky as part of the catalog conversion. With this revised GSC 3.0 in place, BCF performance improved dramatically from the initial ~25% to ~75%.

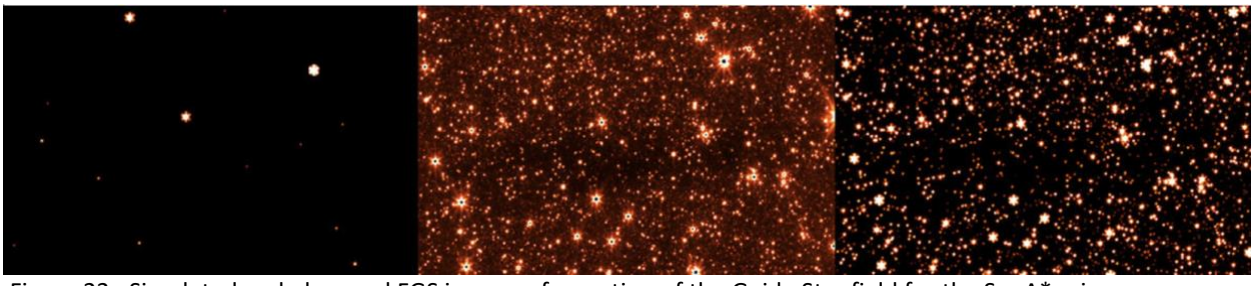

Figure 23: Simulated and observed FGS images of a portion of the Guide Star field for the Sgr A* science program. Simulation based upon the contents of GSC 2.4.3.1 (left); Image captured by the FGS of the same area of the sky (center); Simulation based upon the contents of the GNC, now part of GSC 3.0 (right). These images cover a 48"x33" patch of sky, which is about 8% of the FGS detector area.

While the improvement achieved with this GSC update was significant, there were still many BCF cases where ID mode required several re-tries to find the correct Guide Star, and still failed entirely for some science observations, resulting in lost science. Because the Galactic Center region of the sky is only visible to JWST during a few relatively short durations in each year, some missed science observations might need to wait months before they could be re-scheduled. The FGS overall success rate in ID mode for all regions of the sky is ~96%, so even 75% in BCF regions was not deemed to be satisfactory.

After careful examination of remaining BCF failure cases after the updates made to the GSC, and performing a thorough series of ground-based simulations using the on-orbit image data, it was determined that frequently a commanded Guide Star would not be ranked amongst the 100 candidate bright objects selected by the FGS ID mode bright object scanning algorithm.

This was determined to be due to a peculiarity in the way the FGS algorithm scans through the image data to identify candidate bright objects. In most places in the sky, non-saturated Guide Stars are chosen whose PSFs do not fully saturate a 3x3 pixel window used for calculating star amplitude. However, in BCF regions, there are frequently over 100 stars bright enough to saturate well beyond 3x3 pixels. Once a bright object saturates the entire 3x3 pixel amplitude calculation window in the FGS algorithm, it can only register a maximum of 3x3x25,000 = 225,000 counts (25,000 is the parameterized *satPixelDiffLimit* value which any pixel is assigned if it exceeds the *RawSatPixelLimit* threshold as described in Section 5 of this paper).

Consider Figure 24. A portion of an ID image containing a very bright Guide Star is displayed. The FGS ID images are scanned in a series of 8x8 boxes in order to find pixels which exceed a pixel count threshold to qualify as candidates. This star saturates (indicated by dark red shading) many more pixels than just the 3x3 pixel region used for calculating the star amplitude. Depending on how it lands on the 8x8 scanwindow grid, it may also be broken into several "chunks", which are each evaluated and eventually merged into a single brightest entry in the bright objects list.

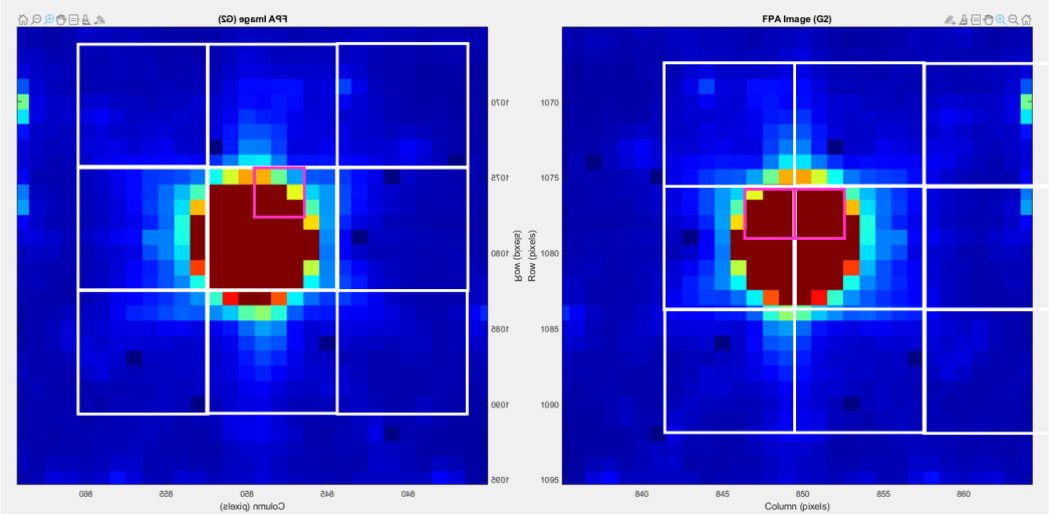

Figure 24: Sample Bright Saturated Star in FGS ID imaging. Left: Star lands "centered" in 8x8 scanwindow grid (white lines) and registers below-maximal 3x3 count sum (pink box). Right: Star lands "split" across 8x8 scanwindow grid (white lines) and at least one 3x3 count sum (pink boxes) may register a maximal 3x3 count sum

However, within each 8x8 scanwindow, the "last" pixel encountered (the order is transposed relative to the images) which exceeds the defined bright threshold is chosen as the center of the 3x3 amplitude calculation box (indicated by pink boxes in Figure 24). For a bright saturated star which is nearly centered in the scanwindow area, such as the case on the left, the 3x3 calculation may then include several non-saturated pixels, and return an amplitude value which is considerably lower than the maximum value of 225,000. Whereas if the same object was split across a

scanwindow, such as at right in Figure 24, there are ways in which a fully saturated 3x3 count sum at the maximum value of 225,000 could be recorded instead by the algorithm. In both cases, this very bright star should ideally be registered at the maximum count sum value of 225,000. However, just due to the random way in which the star is sampled by the scanning algorithm, it may register instead with considerably lower counts, sometimes as low as 140,000.

For BCFs near the Galactic Center, it has been observed that there are many pointings in which more than 100 stars which should produce a fully saturated 3x3 count of 225,000 occur, even within the reduced 12 strip image area in ID mode. But instead of registering 100 objects all with 225,000 counts, the ID algorithm was typically generating bright object lists with varying count sums between around 170,000 and 225,000 counts. And some fully saturated stars with even lower sums were not making it onto the list at all. Sometimes the Guide Star or Reference Stars would thus "fall off the bottom" of the list, and therefore not be available for the subsequent pattern matching stage in identification.

Several methods were investigated for addressing this issue. Ultimately, a method was chosen which involved looping within each scanwindow to find the maximum 3x3 count sum, as opposed to just taking a 3x3 around the first qualifying bright pixel. In this way, a star such as the one pictured in Figure 24 above would always be registered at its full maximum value of 225,000 counts.

Because there are still pointings with more than 100 stars which might generate this maximum count sum in the Galactic Center region, an additional "tie-breaker" feature was added to count up the number of fully-saturated 3x3 sums which occurred for a given candidate star, and to add this tally to the count sum as well. In this way, the resultant bright objects list can be biased to prefer the overall brightest stars in the field. And the Guide Star Selection System can preferentially choose brighter Guide Stars when commanding FGS, in order to ensure that the Guide Star will always make it into the top 100 brightest objects.

These changes required modifications to the FGS FSW code. Note that the ACQ1 mode image processing mimics the scanning method used in ID mode, and so the applied changes affect both ID and ACQ1 modes. An extensive series of validation testing was performed early in 2025, including confirmation that the updated FSW did not cause any problems with FGS operational timing or memory allocation.

This update was implemented as a patch to the FGS FSW onboard JWST in March, 2025. Full evaluation of the achieved performance is underway at the time of writing this paper. It is anticipated based on ground simulations that successful BCF performance exceeding 90% will be achieved. Because of the large number of stars in these fields, it is still unlikely that BCF performance will ever match the full-sky ID performance benchmark of ~96%, since the large number of candidate stars may still produce more pattern matching errors than occur in more sparse star fields. It should also be noted that the FSW update should result in fewer re-tries in ID mode as well, as it becomes more likely that ID will succeed more frequently on its first commanded Guide Star attempt, increasing Observatory efficiency.

9. Possible Future FGS FSW optimizations & Lessons Learned

With the implementation of proposed optimizations to Bright Crowded Field performance as described in Section 8 as of early 2025, remaining areas for potential future FGS performance optimization do still exist. For the most part, these identified areas have been de-prioritized to date, either as having relatively small impact to FGS performance, or due to having very low frequency of occurrence. The effort associated with making changes to the FGS FSW is significant, involving considerable ground-based testing, simulation, and documentation. Uploading patches to onboard FSW introduces risk and affects the overall Observatory availability for performing scientific observations. Therefore, optimizations do need a strong justification in order to be pursued for implementation. Some remaining potential optimizations may be considered more appropriately therefore as "lessons learned" to apply to future

space-based astronomical Observatories. Here are two of the possible future FSW optimizations identified by the FGS instrument team:

1. A known FGS FSW "bug" exists in the process by which the location of the Fine Guide subwindow is determined based on centroids computed during the preceding Track mode. The extrapolation of the window location can use centroids marked as "bad", which may be introduced due to poor quality, or due to the interference of extraneous objects (cosmic ray hits, RTN pixels, or un-mapped bad pixels). This bug has very infrequently interrupted FGS operations, but instances have been recorded, and it is a likely "next fix" for future FSW patching.
2. During FGS operations, the FSW "replaces" mapped bad pixels with an averaged count obtained from that pixel's neighbors. This replacement algorithm is overly simplistic and may under- or over-estimate a Guide Star count rate, which may cause the star to fail its amplitude tolerance checks. A preferred method would be to model expected star PSFs using a fitted Gaussian or other estimate so that a replaced pixel value can be substituted which results in a better overall count rate estimation for affected stars.

In retrospect there are different operational issues with respect to how updates are made in-flight. While the OSS has the capability to change FSW data tables, it would have been less invasive to normal operations to include all the possible configuration parameters needed by the FGS in the original command definitions. The initial command definitions were of course needed in order to define software requirements and hence scope the work. Although a significant effort went into defining the needed FSW functionality up front, there were some known unknowns such as the guider parameters needed to handle bright crowded fields. If these unknowns had been addressed in the development earlier, then it should have been possible to define a BCF ID command for FGS FSW which would have simplified the current Observatory operations.

10. Conclusions

As JWST approaches three years of successful on-orbit normal operations, the series of performance optimizations made to date has resulted in the Observatory nearing its likely ultimate peak level of performance and efficiency. Sufficient time has passed and a sufficient variety of different types of observations in all regions of the sky have occurred now to provide a completely representative view of FGS performance. All the calibrations and improvements implemented to date, as summarized in this paper, have resulted in FGS achieving a remarkable ~96% success rate in achieving closed loop guiding on correctly identified Guide Stars with Noise Equivalent Angle (NEA) typically ≤ 1 mas for GS magnitudes within the FGS sensitivity range, well within all performance requirements.

The improvements to FGS performance made to date, from those planned in advance prior to launch to those discovered during the course of Commissioning and normal operations, have been the result of a concerted effort by the instrument design team and the Flight Operations Team (FOT). Optimizations have been applied at all levels of the system, from ground-based analysis and calibration, to Guide Star Catalog tuning, and even to onboard Flight Software algorithm updates. A very small number of "known" areas for further potential improvement exist, based on the current operational status of the Observatory. These include very low-frequency or low-impact effects which to date have been de-prioritized for optimization efforts, but which may be addressed now that other higher priority impacts have been successfully addressed. The possibility remains that future hardware aging or malfunction will introduce performance degradations which require additional optimizations either in terms of re-calibration or FSW work-arounds. The experience gained in investigating and implementing the optimizations made to date has helped to prepare the FGS instrument team to address any such future needs which may arise.

Acknowledgements

The authors gratefully acknowledge all the other dedicated FGS/NIRISS team members that supported Commissioning:

Loïc Albert, Dave Aldridge, Peter Bartosik, Peter Cameron, Steven Cuturic, Daniel Gaudreau, Fan Gong, Craig Haley, Miranda Link, Michael Maszkiewicz, Alethea Nielson, Kevin Phillips, Aidan Piwowar, Warren Soh, Michel Wander, Andrew Wilson, Carl Wu, Michael Uzzo, Jeff Stys, Lily Liu, Dean Zak, Kyle Elliot, Keira Brooks, Shannon Osborne, Lauren Chambers.

The authors gratefully acknowledge all the other subsystems involved in Commissioning, in particular the Northrop Grumman team for ACS, the Optical Telescope team at Ball Aerospace (now BAE), STScI and GSFC, and all the other leads for Commissioning (Mission Operations Manager, SI leads, Timeline Coordinators, Planning & Scheduling, Science Instrument Teams).

References

[1] Rigby, J., Perrin, M., McElwain, M., et al (623 additional authors not shown), "The Science Performance of JWST as Characterized in Commissioning", 2023, PASP, 135, 048001
[2] Hunter, D. G., "What is it like to operate the James Webb Space Telescope", 2023, 17th International Conference on Space Operations, Dubai, United Arab Emirates, 6 - 10 March 2023, Paper ID #563.
[3] Doyon, R. et al. (65 additional authors not shown), "The Near Infrared Imager and Slitless Spectrograph for the James Webb Space Telescope - I. Instrument Overview and in-Flight Performance," 2023, *PASP* 135 098001 http://www.doi.org/10.1088/1538-3873/acd41b
[4] Maszkiewicz, M., Saad, K., Rowlands, N., Doyon, R. and Hutchings, J. B., "JWST Fine Guidance Sensor and Near-Infrared Imager and Slitless Spectrograph, 2015, Optical Payloads for Space Missions (ed S.-E. Qian), ch35.
[5] Rowlands, N., Warner, G., Berndt, C., Albert, L., Chayer, P., "Pixel classification for the JWST fine guidance sensor", 2012, Proc. SPIE 8453 High Energy, Optical, and Infrared Detectors for Astronomy V, 845313.
[6] Rowlands, N., "JWST FGS tracking performance during the DART observations", 2024, Proc. SPIE 13103 X-Ray, Optical, and Infrared Detectors for Astronomy XI, 131030X. http://www.doi.org/10.1117/12.3020758
[7] Rauscher, B., Boehm, N., Cagiano, S., Delok G. S., Foltz, R., Greenhouse, M. A., Hickey, M., Hill, R. J., Kan, E., Lindler, D., Mott, D. B., Waczynski, A., and Wen, Y., 2014, "New and Better Detectors for the JWST Near-Infrared Spectrograph", 2014, Publications of the Astronomical Society of the Pacific, 126:739–749 https://doi.org/10.1086/677681
[8] Rowlands, N., Beaton, A., Chayer, P., Haley, C., Midwinter, C., Volk, K., Warner, G., Zhou, J., "Updated cryogenic performance test results for the flight model JWST fine guidance sensor", Proc. SPIE 9904, Space Telescopes and Instrumentation 2016: Optical, Infrared, and Millimeter Wave, (2016)
[9] Rowlands, N., Delamer, S., Haley, C., Harpell, E., Vila, M. B., Warner, G., Zhou, J., "Cryogenic performance test results for the flight model JWST fine guidance sensor", 2012, SPIE, 8442-130
[10] Vila, M. B, Lambros, S. D., Diaz, D. M., Fu, H., Lee, S. S., Meza, L., Phillips, K. J., Ben del Rosario, J., Wu, C. "JWST Cryo Fine Guidance Closed Loop Test Results", Proc. SPIE 10698 Space Telescopes and Instrumentation 2018: Optical, Infrared, and Millimeter Wave, 106983R (2018)
[11] Nogueras-Lara, F., Schödel, R., Gallego-Calvente, A. T., Dong, H., Gallego-Cano, E., Shahzamanian, B., Girard, J. H.V., Nishiyama, S., Najarro, F., Neumayer, N., "GALACTICNUCLEUS: A High-Angular-Resolution JHK Imaging Survey of the Galactic Centre", Astronomy & Astrophysics, 631, A20 (2019).